View metadata, citation and similar papers at core.ac.uk

brought to you by CORE

provided by DigitalCommons@The Texas Medical Center

Texas Medical Center Library
DigitalCommons@The Texas Medical Center

UT GSBS Dissertations and Theses (Open Access) | Graduate School of Biomedical Sciences

12-2011

THE EXPRESSION PROFILE OF A GWAS DETECTED GENE (NINJ2) IN THE BRAIN OF A MOUSE MODEL OF ISCHEMIC STROKE

Antonio Joel Tito Jr.

Antonio Joel Tito Jr.

Follow this and additional works at: http://digitalcommons.library.tmc.edu/utgsbs_dissertations

Part of the Medicine and Health Sciences Commons

Recommended Citation

Tito, Antonio Joel Jr. and Tito, Antonio Joel Jr., "THE EXPRESSION PROFILE OF A GWAS DETECTED GENE (NINJ2) IN THE BRAIN OF A MOUSE MODEL OF ISCHEMIC STROKE" (2011). *UT GSBS Dissertations and Theses (Open Access)*. Paper 216.

This Thesis (MS) is brought to you for free and open access by the Graduate School of Biomedical Sciences at DigitalCommons@The Texas Medical Center. It has been accepted for inclusion in UT GSBS Dissertations and Theses (Open Access) by an authorized administrator of DigitalCommons@The Texas Medical Center. For more information, please contact laurel.sanders@library.tmc.edu.

The TMC LIBRARY Health Sciences Resource Center

THE EXPRESSION PROFILE OF A GWAS DETECTED GENE (NINJ2) IN THE BRAIN OF A MOUSE MODEL OF ISCHEMIC STROKE

A

THESIS

Presented to the Faculty of

The University of Texas

Health Science Center at Houston

And

The University of Texas

M.D. Anderson Cancer Center

Graduate School of Biomedical Sciences

in Partial Fulfillment

of the Requirements

for the Degree of

MASTERS OF SCIENCE

By

Antonio Joel Tito, B.S.

Houston, Texas

December, 2011

ABSTRACT

Stroke is the third leading cause of death and a major debilitating disease in the United States. Multiple factors, including genetic factors, contribute to the development of the disease. Genome-wide association studies (GWAS) have contributed to the identification of genetic loci influencing risk for complex diseases, such as stroke. In 2010, a GWAS of incident stroke was performed in four large prospective cohorts from the USA and Europe and identified an association of two Single Nucleotide Polymorphisms (SNPs) on chromosome 12p13 with a greater risk of ischemic stroke in individuals of European and African-American ancestry. These SNPs are located 11 Kb upstream of the nerve injury-induced gene 2, Ninjurin2 (NINJ2), suggesting that this gene may be involved in stroke pathogenesis. NINJ2 is a cell adhesion molecule induced in the distal glial cells from a sciatic-nerve injury at 7-days after injury. In an effort to ascribe a possible role of NINJ2 in stroke, we have assessed changes in the level of gene and protein expression of NINJ2 following a time-course from a transiently induced middle cerebral artery ischemic stroke in mice brains. We report an increase in the gene expression of NINJ2 in the ischemic and peri-infarct (ipsilateral) cortical tissues at 7 and 14-days after stroke. We also report an increase in the protein expression of NINJ2 in the cortex of both the ipsilateral and contralateral cortical tissues at the same time-points. We conclude that the expression of NINJ2 is regulated by an ischemic stroke in the cortex and is consistent with NINJ2 being involved in the recovery time-points of stroke.

ACKNOWLEDGEMENTS

I would like to thank my advisor, Dr. Myriam Fornage, for her mentoring, guidance and support throughout my academic studies and research at UT-Health. I am very grateful for her strong belief of independence and for her valuable advice on excelling in writing and presenting the thesis and the scientific report. I feel I have grown in spirit and wisdom after pursuing a Masters in Science in her lab. I would like to thank Dr. Jaroslaw Aronowski for his mentoring and support during the collaboration as well as members of my committees: Dr. Myriam Fornage, Dr. Jaroslaw Aronowski, Dr. Andrew Bean, Dr. Ba-Bie Teng, Dr. Eric Boerwinkle, Dr. Michael Galko, and Dr. Neal Waxham. Thanks to the members of the lab, especially Dr. Susmita Samanta and Mrs. Ping "Emily" Wang for their mentoring in the project and moral support in the lab. I would like to thank also the administration from GSBS, especially to Dr. Vicky Knutson, and IMM, especially to Mrs. Sonia Davis, for taking time to listen and provide moral support as well as guidance in my academic and research endeavors. This thesis is dedicated to God, my whole family; to my father, Jorge Tito-Izquierdo, Ph.D. P.E. for his belief in education, companionship, and resilience in the moments of hardship; my mother, Elizabeth Tito, for her love, guidance, and companionship and resilience in the moments of hardship; and my girlfriend, Giovanna Fernandez, and brothers, Juan Pablo Tito and Jorge Francisco Tito for their patience and devotion to growing in wisdom and love.

TABLE OF CONTENTS

ABSTRACT ii

ACKNOWLEDGEMENTS iii

TABLE OF CONTENTS v

LIST OF FIGURES vi

CHAPTER ONE – LITERATURE REVIEW 1

Introduction 2

Background on Ischemic Stroke 3

Pathophysiology of Ischemic Stroke 4

Recovery of Stroke 7

Risk Factors for Stroke 7

Genetic Risk in Stroke 9

Genome-wide Association Study 11

Thesis Overview 13

CHAPTER TWO – EXPERIMENTAL METHODS 14

Middle Cerebral Artery Occlusion 15

Harvesting of Mouse Brain Tissues 17

Gene Expression Profiling of NINJ2 after a stroke 19

Gene Expression Analysis 22

NINJ2 Protein Expression after a Stroke 26

CHAPTER THREE – EXPRESSION PROFILE OF NINJ2 31

Introduction 32

Experimental Rationale 39

Results 40

Discussion 56

Conclusion 63

APPENDIX 65

REFERENCES 78

VITA 100

LIST OF FIGURES

Figure 2.1 TTC stained brain tissue sections after a stroke. 18

Figure 2.2 Use of Comparative CT method to determine the Mean Fold Change in Gene Expression. 24

Figure 3.1 Protein sequence, homology, topology, and potential adhesion functions of NINJ2 and NINJ1. 35

Figure 3.2 Protein homology and topology of NINJ2 and NINJA. 36

Figure 3.3 Expression level of human NINJ2 from Northern blot data across normal and cancer human tissues 37

Figure 3.3 Determination of QPCR efficiencies of target gene (NINJ2) and reference gene (RPOL2). 43

Figure 3.4 Pattern of expression of NINJ2 in the ipsilateral and contralateral cortical tissues of MCAo brains. 45

Figure 3.5 Pattern of expression of INOS2 in the ipsilateral and contralateral cortical tissues of MCAo brains 47

Figure 3.6: Detection of the NINJ2 protein at 23 KD by the Protein Tech a-NINJ2 Ab. 49

Figure 3.7: Results from the peptide competition experiment using mouse cortical brain tissue (a) and 293+NINJ2 transfected cell lysates. 51

Figure 3.8: Silver staining of the immuno-purified antigens from the immunoprecipitation experiment with the mouse brain tissue. 53

Figure 3.9: Detection of the 23KD band by immunoprecipitation of the NINJ2 molecules from protein lysates of the 293+NINJ2 transfected cells and mouse brain samples. 54

Figure 3.10:

Changes in the protein levels of NINJ2 in mice brains following a stroke. 55

CHAPTER ONE

Literature Review

INTRODUCTION

Stroke is the third leading cause of death (Lloyd-Jones, D. et al., 2009) and a major debilitating disease in the United States (Hankey, G. and Warlow, C., 1999). It is estimated that every 4 minutes someone dies from a stroke (Lloyd-Jones, D. et al., 2009). This, along with an increase in the population (Thrift, A. et al., 2001), suggest that stroke will continue being a significant financial burden for our economy. Costs associated with stroke are expected to reach a peak of 1.52 trillion dollars by 2050 (Lloyd-Jones, D. et al., 2009). In order to prevent more associated costs from stroke, there is a need to identify the causative factors leading to the development of the disease and address gaps in stroke research.

This thesis reviews the major risk factors for stroke, including genetic risk factors, and the implementation of a Genome-wide Association Study (GWAS) as a tool to identify genes for the disease. It also delineates the major processes underlying the pathophysiology of stroke and some of the conserved mechanisms of brain repair. This thesis will then examine the patterns of expression of a GWAS-detected gene, nerve injury induced gene-2 (NINJ2) in the brain of a mouse used to model a transient ischemic stroke and discuss its potential contribution in the development of the disease. The significance of this work lies in its attempt to follow-up on a hypothesis generated by GWAS about the possible role of the NINJ2 gene in stroke. While GWAS studies have begun to identify genetic loci associated with complex diseases, identification and functional validation of the causal genes and understanding of their molecular mechanisms of action in disease remains a daunting task. It is in light of this that

determining the patterns of gene and protein expression of NINJ2 may provide an insight of its potential contribution to the development of stroke.

BACKGROUND ON ISCHEMIC STROKE

There are two major types of stroke: ischemic and hemorrhagic. Ischemic stroke is most frequent between the two and it is caused by an interruption in the oxygen supply of brain cells (Bonita, R., 1992). Stroke symptoms may involve intense and localized headache, paralysis, speech impairment, and vision loss. The paralysis is on the opposite side of the brain attack if the strike occurs in the left hemisphere of the brain, the paralysis will be on the right side of the body. This is known as contralateral hemiplegia (Good, D., 1990).

The Oxfordshire Classification System of Ischemic stroke subdivides the disease into four subtypes based on the anatomic distribution of the brain infarcts and the associated clinical manifestations (Bamford, J., 1991). The most widely used system of classification in the clinics, however, is known as the Trial of Organization 10172 in Acute Stroke Treatment (TOAST), and it uses the etiology of the disease to classify the subtypes of ischemic stroke (Adams, H., et al., 1993). The TOAST classification system consists of four major ischemic stroke subtype categories. First, cerebral infarctions, also known as athero-thromboembolic stroke, occlude major arteries of the brain, including the Middle Cerebral Artery (MCA), Posterior Cerebral Artery (PCA, and Anterior Cerebral Artery (ACA). The main reason of this major subtype is via an artery-to-artery embolism (Siebler, M. et al., 1994; Fisher, C. and Ojemann, R., 1986). The second subtype is due to small-vessel infarcts that affect deep areas of the brain

(Lammie, G. et al., 1997; Fisher, C., 1979). The third subtype includes the cardio-embolic strokes from other determined etiology such as clots that arise from arteries other than in the brain. The fourth subtype of ischemic strokes involves those that are "cryptogenic," meaning their cause is mostly undetermined (Adams, H. et al., 1993). Each of these subtypes of ischemia constitutes 20% of the total number of cases (Siebler, M. et al., 1994; Lammie, G. et al., 1997, EAFT Study Group, 1993). The remaining 20% of all the cases are of unknown cause (Amarenco, P. et al., 1992).

The advantage of using the etiology for the classification of a complex disease, such as stroke, is that it facilitates the selection of therapies that better manage the outcomes of each subtype of the disease. TOAST has become very useful in studies that require the implementation of standardized subtyping methods of ischemic stroke. For instance, TOAST is used by human stroke studies that aim to determine the genetic contribution with criteria from clinical diagnostic techniques like MRI (Chukwudelunzu, F. et al., 2001). Thus, the accurate classification of variability in the stroke phenotype depends on the consistent organization of the subtypes of the disease.

PATHOPHYSIOLOGY OF ISCHEMIC STROKE

Most of what is known about the pathophysiology of stroke has come from studies performed on cellular excitoxicity (i.e. Kolko, M. et al., 1999), oxidative stress (i.e. Hirsch, E., 1993), mitochondrial dysfunction (i.e. Cedarbaum, J., et al. 1986) and cellular apoptosis (i.e. Heintz, N., 1993). This section outlines some of the major mechanisms underlying the neuropathology of ischemic stroke. These include the disruption of ion homeostasis, reduction of cerebral blood flow, failure of bio-energetics,

disruption of the blood brain barrier, creation of an anaerobic micro-environment, and edema.

Vessel occlusion leads to a reduction in the Cerebral Blood Flow (CBF), or hypo-perfusion to the brain tissue and the generation of an ischemic core. Hypo-perfusion disrupts the delivery of substrates required in the production of adenosine 5'-triphosphate (ATP); thus, quickly leading to a failure in energy generation in the surrounding tissue (Martin, R. et al., 1994; Katsura, K. et al., 1994). ATP depletion activates energy-dependent ion transport channels, including presynaptic voltage-dependent Ca2+ channels (Turski, L. et al., 1998). The intracellular accumulation of Ca2+ ions quickly leads to the depolarization of neurons and glial cells (Martin, R. et al., 1994), followed by the release of excitatory amino acids into the extracellular space (Katsura, K. et al., 1994). Excitoxicity, along with the impediment in the presynaptic reuptake of excitatory amino acids, such as glutamate, signals for the release of reactive oxygen species (ROS) into the postsynaptic cells (McMahon and Nicholls et al., 1990). Membrane permeation by ROS contributes to the disruption of the blood-brain barrier (Dugan, L. et al., 1994). The accumulation of ROS leads to the establishment of an anaerobic environment where glycolysis and lactate production predominate (Nicoli, F. et al., 2003; Brouns, R. et al., 2008). Abnormal anaerobic metabolism in stroke may cause an intracortical infarction in deeper regions of the brain (Brouns R et al., 2008; Uyttenboogaart, M. et al., 2007). This is prevalent especially after a middle cerebral occlusion (Schneweis, S. et al., 2001). These events also lead to the recruitment of activated macrophages to vascular endothelial cells and the subsequent activation of post-inflammatory mechanisms (Zeller, J. et al., 2005; Chong, Z. et al., 2001). The

end result of all of these degenerative processes is micro-vascular injury at the acute phase of a cerebral ischemia (Mohammadi, M., et al. 2011).

Furthermore, the accumulation of injured endothelial cells may induce extravasation of extracellular fluid; thereby causing cytotoxic edema (Shaw, C., et al. 1959; Simard, J. et al., 2010). Cytotoxic edema is primarily due to ATP depletion and the subsequent opening of nonselective cation channels (NC Ca-ATP) (Simard, J. et al., 2010). A large cerebral edema results in the elevation of the intracranial pressure, a shift in the brain tissue, and herniation in the brain tissue near the infarct core (Huttner, H., et al. 2009). The latter is characteristic of a malignant MCA infarction since 80% of patients with brain herniation die (Hacke, W. et al., 1996; Berroushot, J., 1998). Particularly relevant in the prediction of malignancy is an early (within 6 hours of symptoms) detection of edema with perfusion CT and diffusion-weighted magnetic resonance imaging (Thomalla, G. et al., 2003; Thomalla, G. et al., 2010). The ischemic cascades of events are quite traumatic for brain cells, especially for neuronal cell bodies in the grey matter (Turski, L. et al., 1998). The micro-vessel architecture of the brain is such that a severe impairment of blood flow in one major vessel rapidly translates into the irreversible failure of blood supply in surrounding neurons (Turski, L. et al., 1998; Ransom, R. et al., 1990). Moreover, these studies have led to the development of acute phase therapies. However, most of these therapies have failed at the bedside (Cheng, Y., et al., 2004), suggesting a change in the focus of investigation towards an elucidation of compensatory pathways of recovery from a stroke.

RECOVERY OF STROKE

Some phenomena of recovery following a traumatic brain injury have also been shown to contribute to brain repair after a stroke. An example is the co-induction of elements of angiogenic plasticity after brain trauma (Navaratna, D. et al., 2009). It is suggested that enhancement of angiogenic repair and neural plasticity contributes to neural repair and compensation of cerebral blood flow in the stroke penumbra (Thored, P. et al, 2007; Ohab, J. et al, 2006; Taguchi, A. et al, 2004). In fact, some restorative strategies aimed at protecting glial and endothelial function have been shown to induce CBF in the post-ischemic brain tissue (Zhang, Z. et al., 2009).

The “penumbra” consists of salvageable tissue in the brain surrounding the necrotic tissue from the stroke (Wise, R. et al., 1982). The penumbra is first detected minutes after the onset of stroke, but it then becomes progressively worse as time passes by (Kaplan, B. et al., 1991). The most adequate time for the reestablishment of CBF in the penumbra is within the first 2 to 5 hours after the onset of stroke (Jones, T. et al., 1981; Kaplan, B. et al., 1991). Therefore, it is crucial that for the design of a cellular treatment for stroke, not only should we explore the fundamentals of cell death processes but also determine the activation of intrinsic mechanisms underlying tissue repair in the stroke penumbra (Lo, H. et al., 2003).

RISK FACTORS FOR STROKE

It is of interest to determine the key factors that predispose certain people to the disease. Determining the cause of these factors stroke (Khaw, K., 1996) and treating them at an early stage (World Health Report, 1999; WHO Monica Project, 1988) is

expected to significantly reduce the incidence of stroke. One major causative risk factor of stroke is an increase in the levels of diastolic blood pressure (DBP). In a landmark study by McMahon et al. (1990), the direct contribution of high blood pressure to an increasing risk for stroke was established. This study followed up on a Framingham study that first linked hypertension with an increase in the incidence of ischemic stroke (Kannel, W., et al. 1970). The McMahon prospective cohort study demonstrates a cumulative risk of incidence of stroke in patients with high levels of DBP. It has been reported that treatment of vascular risk factors in hypertensive patient groups at high risk of developing a stroke confers a proportional reduction in the incidence of stroke (Wolf, P. et al., 1991). In general, a modest reduction in DBP levels significantly reduces stroke incidence, especially in the aging population (McMahon et al. 1990). These observations would forever change an erroneous concept that stated that the reduction in CBF precipitates ischemic stroke in the elderly suffering from low blood pressure (Wolf, P. et al., 2000). Furthermore, these seminal studies served as the foundation for clinical trials using at-risk patient populations, including the Perindopril Protection against Recurrent Stroke Study (PROGRESS Collaborative Group, 2001). In the PROGRESS study, it was suggested that a modest reduction in the DBP level from population-wide and at-risk population groups confer benefits to the reduction of neurological deficits of stroke, such as dementia (Ott, A. et al., 1998; Liao DP et al., 1996; Skoog, I., 1993).

Other causative risk factors of stroke, apart from hypertension (Kannel, W., et al. 1970; MacMahon, S., et al., 1990), include a history of a previous transient ischemic attack (Bamford, J. et al., 1991) and/or other cardiovascular diseases such as diabetes

mellitus (WHO Expert Committee on Diabetes Mellitus) and atrial fibrillation (Hart et al., 1999). There are also other risk factors of stroke that confer an increase in the overall risk of stroke (McMahon, H. et al., 1990). For instance, large BMI due to an unhealthy lifestyle and lack of exercise (Hu et al., 2005 and 2007), smoking (Mancia, G., et al. 1990), and high carbohydrate diet (Chiba, T. et al., 2009) may complicate the risk of stroke.

GENETIC RISK IN STROKE

Stroke is a multifactorial and complex disease. Nevertheless, there is also substantial data that suggest genetic component underlying stroke susceptibility (Turski L. et al., 1998). In fact, a Framingham study in the 1970s first reported a significant risk of developing the disease in people with a parental history of stroke, suggesting a familial contribution to the risk of stroke (Kannel, W.B. et al., 1970). Later in the 1990s, Kiely et al. followed up on this study using data consisting of familial aggregation of stroke. The Kiely et al. study reported a direct association between parental history of stroke and increased risk of stroke (Kiely, D. et al. 1993); an observation that would then be confirmed in the Family Heart Study (Liao, D. et al., 1997).

A twin study performed by Brass et al. (Brass, L. et al. 1992), and later confirmed in a study by Bak *et al.* (Bak, S. et al., 2002), also provides strong evidences for genetic risk in stroke. The primary role of twin studies is to distinguish between shared family effects without a genetic contribution from those that do arise from genetic effects. A twin study usually involves comparing monozygotic (MZ) twin pairs with dizygotic (DZ) twins. MZ twins share all of their genes while DZ twins only share half of their genes.

Twin studies use the concordance rate to determine the genetic contribution to the development of a disease (McGue, M., 1992). A study showing MZ and DZ twins having 100% and 50% concordance rates, respectively, constitute a complete genetic determination for the disease (MacGregor, A. et al. 2000). Results from the Brass *et al.* study report a 17.7% for the concordance rate in MZ and 3.6% concordance rate in DZ twins, suggesting a significant genetic predisposition to stroke (Brass, L. et al., 1992). Furthermore, there is a central assumption in twin studies that calls for an equal environmental exposure by both MZ and DZ twins (Kendler, K., et al. 1993; Guo, S. 2001). Yet, this assumption may not always be true. If the concordance rates for both MZ and DZ twins are similar to each other, then an environmental rather than a genetic effect is to be suggested (Risch, N. 2001). For instance, a later study by Brass reports there is an additive environmental effect as the patients increase in age (Brass, L., 2000), as it is to be predicted from the similarity in the concordance rates between the MZ and DZ twins from the first study.

However, much of what has been learned about the genetic of stroke has come from studies on single gene Mendelian disorders associated with stroke. One example is Cerebral Autosomal Dominant arteriopathy with Subcortical Infarcts and Leukoencephalopathy (CADASIL) (Joutel, A. et al., 1997). CADASIL is characterized by a progressive disruption of the vascular endothelium and thrombosis, both of which manifest among subpopulations of stroke (Ruchoux, M. et al., 1998). And yet, there is a limit in determining a genetic risk in the general population from single gene disorders. People with CADASIL, for instance, do not respond to the regular treatment plan with tPA used for the other subtypes of stroke (Viitanen, M. et al 2000). Consequently, a

treatment originally designed for the single-gene disorder may not necessarily work for the treatment of other subtypes of stroke. Thus, it can be suggested that the genetic contribution of a single-gene disease is not sufficient for the development of all other types of stroke. Hence, it is necessary to implement a genome-wide approach to find genes that may be linked to stroke.

GENOMEWIDE ASSOCIATION STUDY (GWAS)

Novel methods from genetic epidemiology, such as genome-wide association studies (GWAS), have contributed to the genomic analysis of complex diseases (Hanis, C., et al. 1996; Collins, F. et al. 1997). GWAS studies are commonly designed using either retrospective case-controls or prospectively multi-national cohorts. In a case-control study, samples are taken from diseased subjects at medical care centers, together with samples from age and gender matched control subjects. Cohort studies consist in sampling all the members of a population, regardless of age or gender. A GWAS analyzes millions of SNPs from multi-national cohorts with large sample sizes of diseased and healthy people enrolling into the study. The study consists of determining the frequency of SNPs in the healthy population and comparing it with the frequency in the diseased population. A p-value is assigned to every SNP and a significant difference from the norm is reached when the p-value is lower than a pre-specified threshold (Manolio, T., et al. 2010).

Thus, a GWAS study provides the association of SNPs with the disease as well as genes in close proximity with the associated SNP (Tu, I. and Whittemore, A., 1999). These genes, however, are not necessarily the cause of the disease since a GWAS

study is based on the principle of linkage disequilibrium (LD) (Manolio, T., et al. 2010). The underlying assumption of LD is that the physical distance between the genetic marker and the disease gene is small enough to demonstrate an allelic association at the population level (Weiss, K. 2002). Most associations usually represent a susceptible locus that increases the chance of developing the disease (Greenberg, D. 1993). Furthermore, the GWAS approach has had success in identifying associations of genetic markers with complex conditions such as diabetes, cardiovascular abnormalities and Parkinson disease (Johnson, A. et al. 2009). To date, there has not been many GWAS studies published on the genetics of stroke. In fact, the first GWAS study ever published in ischemic stroke is from Matarin et al. in 2007. The case-control study from Matarin et al. did not reveal any locus that contributes to a higher risk in the development of ischemic stroke (Matarin M. et al., 2007). The major limiting factor of this study is its small sample size, followed by the use of a control design with large survival and selection biases.

In 2010, a GWAS study is performed with four large prospective cohorts from the USA and Europe. These cohorts are all part of an international consortium known as the Cohorts for Heart and Aging Research in Genomic Epidemiology (CHARGE) (Psaty, B. et al., 2009). Overall, the CHARGE consortium contributed with a sample size of 19,602 participants of European ancestry followed prospectively over an average period of 11 years (Ikram, M. et al., 2010). A total of 1544 incident strokes developed over the follow-up period. 1164 of these are ischemic strokes. In this study, stroke is defined with the WHO definition as stated above (WHO, 1999). The types of stroke studied are ischemic, hemorrhagic, or “unknown,” all assessed by clinical and imaging

criteria. Ischemic stroke is further subdivided into the atherothrombotic and cardioembolic subtypes (Ikram, M. et al., 2010). The GWAS identified an association in two Single Nucleotide Polymorphisms (SNPs) on chromosome 12p13 with a greater risk of ischemic stroke in individuals of European and African-American ancestry. These SNPs are located 11 Kb upstream of the NINJ2, suggesting that this gene may be influencing stroke risk.

THESIS OVERVIEW

This thesis reports changes in mRNA and protein levels of NINJ2 following a transient focal cortical ischemic stroke in mice using a middle cerebral artery occlusion (MCAo) model. This is done in order to determine whether NINJ2 is involved in ischemic stroke.

CHAPTER TWO

EXPERIMENTAL METHODS

MIDDLE CEREBRAL ARTERY OCCLUSION (MCAo)

Background

The implementation of a well-designed biological model in mice is crucial for a quantitative study of the differential gene expression in the diseased state. Animal models for neurodegenerative diseases have revealed some of the mechanisms underlying risk factors of disease (Bacigaluppi M., et al. 2010). Three of the major caveats of animal models of stroke are high mortality rate and low reproducibility in determining disease mechanisms (Garcia-Bonilla L. et al., 2011). We perform a transient Middle Cerebral Artery occlusion (MCAo) in 9-10 weeks old male wild-type C57BL/6 mice. The stroke is focal to the cortex and reproducible between animals. The advantage of using this animal model is that it reduces the death rate of mice and increases reproducibility of the biochemical studies from brain tissues. In the case of the transient stroke mouse model, replicating the same degree of necrosis across all brain tissues depends on the time in which the mice are subjected to the stroke as well as surgeon's skills in performing the surgery. The tandem and reversible induction of ischemic stroke also permits for the visualization of the penumbra in a mouse's brain. Extracting tissue from the penumbra is required for the detection of changes in expression of genes that may be involved in the recovery phases of a stroke.

Transient MCAo Induction – Mr. Roger Strong, in collaboration with Dr. Jaroslaw Arnowski, induced a focal ischemia following a left middle cerebral artery (MCA), and left common carotid artery (CCA) transient occlusion scheme as summarized below (Waxham, M. et al., 1996). A day before the surgery, an overnight starving order is

placed for a maximum of five mice per day. On the day of the surgery, mice are taken to the surgery room where they are weighed and anesthetized with chloral hydrate (350 mg/kg). The temporal side of the mouse's head as well as its neck is barbed while the mouse remained unconscious. The surgical procedure started by making a small burr hole with a surgical electrical hand-drill over the MCA without touching any of the cerebral arteries and causing intracranial bleeding. Once the MCA is exposed under the magnification of an inverted microscope, a 3 mm stainless steel wire is inserted "underneath the MCA rostral to the rhinal fissure, proximal to the major bifurcation of the MCA, and distal to the lenticulostriate arteries" (Waxham, M. et al., 1996). The artery is then pushed towards the cortex and then rotated counterclockwise. Immediately after, the common carotid artery is occluded using autramatic Heifetz aneurysm clips in order to facilitate the transient induction of a cortical stroke.

Measurement of Cerebral Blood Flow (CBF) – CBF is measured prior to and immediately after placing the subcortical wire in the mouse brain using a laser Doppler flowmeter. 90 minutes after the surgery, the CBF is reperfused into the brain by removing the aneurysm clips from the CCA, rotating the wire counterclockwise on the MCA, and removing the wire from the brain. CBF is then measured again.

Body Heat Regulation – The mouse is placed on top of a warm plate throughout the duration of the procedure in order to maintain the body temperature at the physiological level of 37°C +/- 0.5^{o}C. The feed-forward temperature controller, coupled to a heating lamp and a warm plate are used to maintain a stable core body temperature (Waxham, M. et al., 1996).

Mouse Care – Mice arrived from Jackson Laboratory and left to acclimatize at room environment of the Animal Care Facility over a period of 3 days. In the meantime, mice are fed with standard mouse diet and housed in standard mouse cages on a 12 h inverted light/dark cycle. All experimental procedures are approved by the Institutional Animal Care Committee of University of Texas Health Science Center at Houston at the Medical School.

HARVESTING OF MOUSE BRAIN TISSUES

Experimental Timeline for Brain Extraction – The time points of brain extraction are 0 hours, 3 hours, 24 hours, 7 days, and 14 days after stroke. 3 mice are randomly taken from each group in the timeline of experiments. A mouse is removed from the cage and anesthetized. The mouse's heart is then perfused with ice cold PBS following the approved animal protocol for perfusion. *Tissue Dissection*– Mice brains are dissected in such a way that the cortex is preserved with the least amount of time spent at room temperature (RT). The time allowed for brain tissue to be at room temperature is of less than 30 seconds in order to preserve the functional stability of proteins. The brain is placed on a brain dissecting mold and sterile blades are used to cut 2-3 mm of the brain tissues. The isolated brain is quickly washed with ice cold 1X PBS pH 7.4, carefully dried with a damped paper towel, placed on a brain mold, cut into the corresponding sections, and dissected on a petri dish with cold PBS. Figure 2.1 shows an example of the tissue sections stained with TTC.

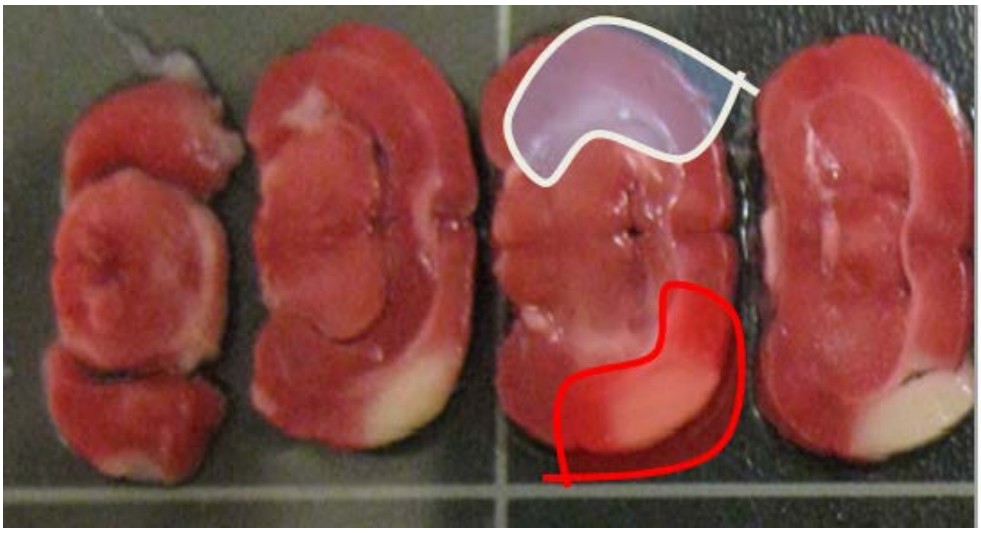

Figure 2.1 TTC stained brain tissue sections after a stroke. Dissected 200um sections of a mouse brain 24 hours after a transient Ischemic stroke of 90 minutes. These sections are stained with TTC for mitochondria. The red line in this figure outlines the necrotic cortical tissue, namely the ipsilateral tissue, and the penumbra. The blue shadow represents the contralateral tissue. Both the ipsilateral and the contralateral tissues are cut in the same size.

Cortex Extraction – A surgical knife is used to dissect the brain into two hemispheres, keeping the injured hemisphere on one side. The cortex is then removed with a blunted knife by making an incision through the corpus callosum. The cortex consists of the outermost brain tissue. A small piece from the cortical tissues of each hemisphere is harvested for the biochemical studies, as shown by the demarcations in figure 2.1.

Sample identification and preservation – Once the tissue dissection is made, the cortical and striatal tissues are preserved in eppendorff tubes labeled as followed: 1 for injured cortex, 2 for contralateral cortex, 3 for injured striatum, and 4 for contralateral striatum. Once all the brains are extracted and placed at -80°C for at least 24 hours, they are then ready for homogenization.

GENE EXPRESSION PROFILING OF NINJ2 AFTER A STROKE

RNA Isolation – Total RNA is isolated from each brain tissue using the Trizol method. Basically, 1 ml of Trizol reagent (Gibco-BRL) is added onto glass test tubes to homogenize the brain tissues. The cortical tissues are added one by one from the -80°C stock onto tubes containing the Trizol reagent. The plastic pistol is moved up and down the test tube 6 times for 10 seconds each. The tissue is placed on ice for 40 minutes until a stringy-like material appeared. 1/10 volume of chloroform (99% stabilized with chylenes) is added to it. Samples are vortexed for 15 seconds vigorously and left on ice for 5 minutes. Samples are then spun down in a microfuge at 13.2 rpm for 20 minutes at 4°C. The top layer (clear) is carefully transferred into a new RNAse free eppendorf tube and 1/10 volume of 3M sodium acetate is added to it, followed by the same volume (55µl) of Isopropanol. The solutions are gently inverted to mix. Samples are spun in a microfuge at 13.2 rpm for 30 minutes at 4°C. RNA is seen as a nice white pellet at the bottom. The pellet is then washed with 70% cold ethanol (made by diluting into DEPC-treated water). Diluted samples are centrifuged in microfuge at 13.2 rpm for 5 minutes at 4°C. Supernatant are removed and the samples are left to dry. The pellet containing the RNA is air dried for 10 minutes. Pellet is dissolved in 70 µl of DEPC-treated water and samples are heated for 10 minutes at 60oC to help dissolve RNA. RNA concentration is measured at 260 µm using a nanodrop (Aronowski Lab Protocol). Once the RNA is extracted from the tissue homogenate, the cDNA is synthesized in order to determine changes in gene expression.

RNA-cDNA reaction – Reverse transcription of the RNA samples into the cDNA are prepared in the following manner. The High Capacity RNA-to-cDNA Kit (Part # 4387406) components are allowed to thaw on ice. The lab bench areas as well as the gloves are cleaned thoroughly with 70% Ethanol and RNAse ZAP in order to remove any potential contaminant on the surface. An RNA aliquot is removed from each brain sample placed in the -80°C freezer and placed on ice. The RNA aliquots are prepared so that the final concentration yields 0.25 µg/µl per sample. The RNA-to-cDNA reaction involves using 1ug of RNA. 4 µl of the RNA aliquot is filled to a total of 10 µl volume with 6µl of nuclease free ddH2O. The diluted RNA solutions (1ug total) are heated to 70°C for 10 minutes in order to destroy secondary RNA structures. The 2X RT Master Mix is also prepared on ice using the components from the RT Kit and following the instructions indicated in the appendix. 10ul of the 2X RT Master Mix is added into the heated RNA solutions (total volume of 20ul). The tubes are sealed and briefly centrifuged to spin down contents and eliminate bubbles. It is assumed that for every microliter of solution in the RNA-cDNA reaction tube, 1000 ng or 1 µg of cDNA molecules are produced. The complementary DNA (cDNA) molecules produced in the first step of the reaction serves as the template for the qPCR reaction. The qPCR reaction is the second step after the synthesis of the cDNA. DNA is more stable than RNA and the relative number of cDNA molecules produced in the first step of the reaction by the RNA polymerase is directly proportional with the number of RNA molecules present in the sample.

Quantitative Polymerase Chain Reaction (QPCR) – We implement qPCR to quantify changes in gene expression following a stroke in mice brains. The basis for qPCR

consists in the use of Taqman chemistry, consisting of a fluorescent probe attached to a chemically synthesized DNA primer. The taqman probe contains two molecules: a fluorophore and a quencher. As the DNA polymerase extends forward in the DNA, the fluorophore is separated from the quencher and it releases a fluorescent signal that is read by the machine. The primer is complementary to a conserved DNA sequence in the gene of interest onto which the DNA polymerase binds to and mediates cloning of the DNA. Commercially available primers are used for NINJ2, RPOL2, and INOS2 with sequences evaluated for transcript specificity, genomic DNA specificity, and other functional considerations as stated in the appendix.

Plate Design – A flexible template in Microsoft Excel is created for the analysis of the raw data. An example of this template is shown in the appendix (A1). Basically, each plate carries both the target and endogenous gene probes, along with the cDNA samples from tissues of the control and experimental brains. The target gene is added to the top 4 rows, followed by the endogenous genes on the bottom 4 rows. The experiments are designed such that the whole time-line of expression would fit into two plates named as Injury and Recovery plates. Both plates shared a group of samples consisting of cDNA from mice sacked at the 3rd day after the stroke. This serves as an internal control to lower the inter-assay variability between experimental runs.

Standard Curve – A standard curve is generated for every qPCR plate using cDNA from the cortical tissue of a healthy mouse brain used as a naïve sample in the experimentations. There are usually two to three serial dilution points in each standard curve. The reason for incorporating the standard curve is to calculate the qPCR amplification efficiency and also keep a control on the quality of qPCR reagents.

Independent sets of standard curves are also prepared for each probe using a larger number of dilution points.

GENE EXPRESSION ANALYSIS

Introduction to Methods of Analysis – There are two main methods of presenting the gene expression data from quantitative Polymerase Chain Reaction signals (qPCR): absolute and relative quantification. In the absolute quantification method, the copy number of the gene is calculated using a standard curve. The standard curve transforms the qPCR signal to an exact copy number (Chen C et al., 2005). Absolute expression is necessary when presenting a precise quantity of amplicon. The disadvantage of absolute quantification is its strict dependence on standard curves for data analysis. In this section of the chapter, the method followed for the relative quantification of changes in NINJ2 gene expression in brain tissues is explained. The selection process of the endogenous gene and the basic mathematical assumptions for all these calculations, including the calculation of the qPCR amplification efficiency, are also explained.

Amplification Data – The qPCR reaction generates a log-linear plot of the fluorescence signal versus the cycle number. The endpoint of the qPCR analysis is defined by a threshold cycle (C_T) value and it represents the exponential phase of the PCR amplification of the gene. The C_T value is inversely proportional to the amount of amplicon in the reaction. Given the exponential nature of the C_T terms, the use of raw C_T values is avoided in the tests of statistics as well as for Relative Quantification (RQ) calculations (Livak K. and Schmittgen, T., 2001).

Comparative Ct method for Data Analysis – The comparative Ct method, also known as the $2^{-\bullet\bullet}{}_{T}$ method, is also implemented for the conversion of the C_T values into normalized relative quantities. This method is followed since it permits the analysis of low input RNA from cortical tissues. This method is derived from a mathematical model developed by Livak and Schmittgen (Livak K. and Schmittgen, T., 2001). Results from this method yield the fold induction in NINJ2, normalized to RPOL2 and relative to the average expression of the RQ values of all three mice at time zero. The calculations are performed with the RQ values of three mice per time-point repeated in three experimental runs. First, the mean of the CT values corresponding to the technical replicates of each sample is calculated. Then, the mean CT at time point zero for the target and endogenous genes are calculated. Then, the CT value of the target gene of each technical replicate is subtracted minus the CT value of the endogenous gene of the corresponding sample. The mean CT value at time 0 of the target gene is then subtracted from the mean CT at time 0 of the endogenous gene. The ddCT value is computed for each technical replicate by subtracting the two values. The 2-ddCT is computed from 2 to the negative power of the resultant value. Calculations are performed for each qPCR experimental run.

SUM =2^-((G5-G43)-(I5-I43))

	A	B	C	D	E	F	G	H	I	J	K	L	M	N	O
4	Sample	Well	Type	Gene	Time	Primer/ Probe	Ct TimeX	Mean CT	Mean CT Time 0	2^-ddCT	Mean Fold Change in Gene Expression				
5	1	A10	UNK	ninj2	naïve	PR1	30.583778		30.25217138	=2^-((G5-G43)-(I5-I43))					
6	2	A11	UNK	ninj2	naïve	PR1	30.419127	30.5557317	30.25217138	1.231623564					
7	3	A12	UNK	ninj2	naïve	PR1	30.66429		30.25217138	1.00502708	1.12806353				
8	4	B10	UNK	ninj2	naïve	PR1	29.608494		30.25217138	0.820183926					
9	5	B11	UNK	ninj2	naïve	PR1	29.610102	29.582872	30.25217138	0.848271135					
10	6	B12	UNK	ninj2	naïve	PR1	29.53002		30.25217138	0.813599318	0.82735146				
11	7	C10	UNK	ninj2	naïve	PR1	30.79077		30.25217138	1.124734414					
12	8	C11	UNK	ninj2	naïve	PR1		30.80078							
13	9	C12	UNK	ninj2	naïve	PR1	30.81079		30.25217138	1.105783059	1.115258737		1.023557909		
14	10	A1	UNK	ninj2	3days	PR1	31.572649		30.25217138	0.762867483					
15	11	A2	UNK	ninj2	3days	PR1	31.498148	31.489687	30.25217138	0.936868439					
16	12	A3	UNK	ninj2	3days	PR1	31.398264		30.25217138	0.862615996	0.854117306				
17	13	B1	UNK	ninj2	3days	PR1	30.525415		30.25217138	0.743601391					
18	14	B2	UNK	ninj2	3days	PR1	30.582146	30.5537805	30.25217138	0.855579829					
19	15	B3	UNK	ninj2	3days	PR1					0.79959061				

Figure 2.2 Use of Comparative CT method to determine the Mean Fold Change in Gene Expression.

Implementation of the 2^{-} $_{T}$ method for the Endogenous Gene selection – The effect of experimental treatment (MCAo stroke) on the expression of the endogenous reference is studied using the 2^{-} method, a derivative of the *2$^{-\bullet\bullet}$ $_{T}$* method. The 2^{-} method converts the CT values from the exponential to the linear form, thus permitting the validation of the candidate internal control gene (RPOL2). Validation consists in determining the effect of the experimental treatment on the expression of RPOL2 (Livak K. and Schmittgen, T., 2001). The same concentrations of input RNA are used to generate cDNA for all the reactions, as shown in the appendix.

Amplification Efficiency – The qPCR amplification efficiencies for the target (NINJ2) and control (RPOL2) genes are calculated according to equation 1. The underlying assumption of the efficiency calculation is that it is “assay dependent and sample independent” (Hellemans J. et al., 2007). Thus, the amplification efficiencies are calculated using aliquots of cDNA isolated from cortical tissues of naïve mice. The amplification efficiency is determined with a linear regression of a serial dilution series from known quantities of cDNA concentrations.

Eq. 1:

The efficiency values are converted to percent efficiencies using an equation (Eq. 1a) derived from Eq. 1.

Eq. 1a:

This experimental design permits the analysis of the amplification efficiencies for both target and endogenous probe assays. Equal qPCR amplification efficiencies are determined by (Perkin Elmer and Pfaffl M. 2001). This is the initial presumption for the delta-delta Ct method to hold true (Ruijter J.M. et al., 2009). It can be suggested that, under this condition, both target and reference probes are selective for their complementary sequence in the gene of interest. It also suggests there are no inhibitors in the reaction from the RNA isolation process (Perkin Elmer).

Statistics – A total of 3 replicates of the experiments are performed with 3 animals per experiment, representing the three time-points following stroke. All analyses are conducted using SAS9.2 statistical software. Data are analyzed using a mixed model to account for the correlation between the replicate experiments. Gene expression levels are modeled as a function of time groups and experiment groups with repeated measures on the latter group. Covariance structure for the repeated measurements is modeled as unstructured. Pairwise differences in means between time points are tested using a t-test. P values are corrected for multiple comparisons using a Tukey-Kramer procedure.

NINJ2 PROTEIN EXPRESSION AFTER A STROKE

Lysis Buffer Preparation – The purpose of this section is to detect NINJ2 protein in tissues of brain from mice with a commercially available antibody. The commercially available antibodies reported various molecular size for NINJ2, thus a gradient gel is used to determine changes in signal levels across a whole range of molecular sizes.

The mouse brain and lung tissues are used to determine changes in the level of NINJ2 proteins following a stroke. The lung tissue is used since it is where NINJ2 is highly expressed. The highest expression of the NINJ2 gene is in the mouse lung (Milbrandt et al., 2000). For this, a lysis buffer is needed to prepare the tissues for protein analysis. The lysis buffer used is the regular RIPA (pH 7.0) buffer stated on appendix B. This RIPA buffer uses a mild detergent that disrupts the cellular membranes in the tissue and preserves proteins in micelles. It also provides the necessary reagents that resembles the physiological state of the cell and reduces the mechanical stress to the cellular contents caused by the homogenization process. Prior to homogenization, 1 µl each of the Protease inhibitor and Phosphatase inhibitor (1X) are added into the RIPA buffer. This step disrupts the enzymatic action of the cellular proteases and phosphatases released into the solution.

Tissue homogenization – The tissue samples in the RIPA buffer are lysed about a minute in the following manner. The tissues are given 6-8 strokes in a glass tube using a Teflon homogenizer, preventing foaming on the top. The Teflon homogenizer is used instead of the douncer homogenizer in order to minimize protein disruption. The

homogenates are separated into multiple eppendorff tubes while kept on ice. In order to prepare aliquots of the supernatant for analysis, some of the initial aliquots are centrifuged at max speed (~14,000 rpm) for 10 minutes. The supernatants are stored in the form of small aliquots and the whole homogenates are also saved for protein sampling. 10 µl of each of the supernatant aliquots are saved for protein quantification. Prior to removing samples from each aliquot, the aliquots are carefully shaken using a vortex in a speedy manner so as to prevent protein degradation. Brain and lung lysates are not thawed and frozen more than 2 times in order to prevent loss in the degree of structure preservation.

SDS-PAGE – The tissue samples are treated with 1X Loading Buffer (1:1) at RT before running them in the gel. The loading buffer is prepared as a 4X stock and diluted to a 1X running solution as shown in the appendix. 15 µl of each sample, containing 80 µg of protein, are diluted in a total volume of 20 ul with RIPA buffer. To make 20 µl of the final solution, 6.6 µl of the 4X sample buffer stock is added on the sample, diluting it into a final concentration of 1X. Once the samples are mixed with the loading buffer, these are then processed for the protein gels.

Although the heating conditions varied, an optimized heating temperature is provided to separate the NINJ2 protein from the rest of the proteins in the sample pool. This consisted in heating the samples at 60°C for 20 minutes during the electrophoretic run. The mild heat and long-time process of sample preparation prevents unnecessary protein aggregation caused by inducing hydrophobic proteins to conglomerate in boiling conditions. The membrane domain of NINJ2 consists mostly of hydrophobic residues, making it easy to aggregate at near-boiling temperatures. The 12% gels are casted

using the protocol from Aronowski Lab as shown in the appendix. The 12% gel is used to separate the mid-range molecular size proteins (12-50Kd). The premade Invitrogen gradient gel is also used to confirm the results. The procedure for running an electrophoretic gel is summarized in the appendix.

Protein transfer – The procedure for the transfer of negatively charged proteins onto the positive charged pvdf membrane is explained in the appendix. The protein transfer differs from the norm in that it has to be done overnight at 25Volts and at 4oC.

Antibody Incubation –The PVDF membrane is first blocked with a blocking buffer consisting of 0.5 g of powder milk in 10 ml of TBSt. This is done for 1 hour with gentle shaking. The membrane is then rinsed with wash buffer before antibody incubation. The antibodies used for the selection of the NINJ2 antigens in the tissue homogenate (immunological incubation) have rabbit-derived IgG heavy chains and light chains with motifs specific against mouse sequence. This antibody is acquired from Protein Tech Inc. This antibody is selected after having failed with multiple other antibodies that gave a significant amount of background and non-selective identification of proteins in the sample. The starting dilution of the P. Tech antibody is 1:200 and the final dilution factor is 1:1000; yet the optimal dilution factor is that of 1:500. All of these dilutions are done in the blocking buffer. The antibody incubation and film developing procedures are shown in the appendix.

Selectivity of Antibody – The purpose of stripping the membrane is to confirm the immunoreactivity of the Antibody. This is done by incubating the same membrane with different dilutions of the antibody and stripping the antibody with the stripping solution as

shown in the appendix. The same membrane is incubated with another antibody, including the antibody provided by Milbrandt. This allows one to cross-check the results seen at the level of protein's molecular size reported in the literature. *Peptide competition assay* – The purpose of this section is to use a peptide that is specific against the protein of interest and, thus, block the binding of the primary antibody. The peptide designed by Santa Cruz (sc-79653) maps the membrane domain of the protein. The Protein Tech Company antibody is used for the reaction. The peptide competition experiment is performed using a 200X molar ratio of peptide to antibody in order to compete for the specific binding site in the antibody. The peptide sequences are designed to be the same as the membrane domain of the mouse NINJ2 protein. The peptide and antibody solutions are mixed in the blocking buffer solution at 4oC overnight before using them to incubate the membrane containing the protein lysate from the brain, lung, and NINJ2 transfected 293+T cells samples (Santa Cruz). Overnight incubation is done in order to expose the antigenic site of the antibody longer with the NINJ2 in solution. Results for the brain, lung and 293+T cells are shown in figure 3.8. A negative control is also run using water instead of peptides for both experiments. 200 fold of molar excess of NINJ2 peptide is prepared in the same solution. 4 ug of the peptide (0.2 ug/ul stock) and 0.2067 ug of primary Antibody (0.2066 ug/ul stock) are used for the preparation of the 200X peptide to antibody solution. The blocking buffer (5% milk and 1% tween 20) is used as the diluent for the solution. A control sample is prepared using water instead of the antibody. A membrane strip containing the protein is incubated with the peptide/antibody solution overnight at 4°C. A control membrane strip from the same protein is also incubated with the peptide/water

solution overnight at 4°C. A secondary antibody attached to horseradish peroxidase is used to develop the membrane with a chromogenic substrate.

Immunoprecipitation using Protein G Magna Beads –The purpose of using the magna beads covalently linked to Protein G is to separate the protein of interest from the pool of 1 ug of proteins in the supernatant of a brain tissue homogenate. The beads are composed of silanized iron oxide, so they are surrounded by an external magnetic field that is also super paramagnetic, with no magnetic memory (Thermo Scientific 21348). This means that when a magnet is used, along with other non-disruptive chemicals, the protein of interest (antigen) will become purified from the tissue culture. First, the 1:500 of the glycerol-based Protein Tech anti-NINJ2 antibody is mixed with 1gram of tissue lysate from brain samples at 4°C overnight. Then, the IgG magnetic beads are incubated with the solution containing 0.4ug of the Protein Tech anti-human NINJ2 antibody at Room Temperature for 1 hour. The protein G molecules on the surface of the beads link the heavy chains of the antibodies using affinity binding. The antigens and antibodies are then dissociated from the beads with an elution buffer consisting of a low-pH elution buffer (1M Glycine pH 2.4). The purpose of using this elution buffer is to separate the antigen from the complex without also obtaining a signal from the antibody. Once proteins are eluted out from the solution, The glycine elution is then mixed on a 1:1 ratio with the RIPA buffer. This was placed in the Laemmli buffer and heated at 60°C for 20 minutes prior to loading into the protein gel. 0.08ug of P.Tech a-NINJ2 antibodies in blocking buffer is then used to detect the precipitated NINJ2 antigens from the elution.

CHAPTER THREE

EXPRESSION PROFILE OF NINJ2 AFTER A STROKE

INTRODUCTION

A GWAS study reported two SNPs, rs11833579 and rs12425791, 11 kilo-bases upstream of NINJ2 associated with the risk of ischemic stroke, suggesting NINJ2 is a candidate gene for stroke (Ikram et al., 2010). These SNPs are not necessarily the causal variants for the disease. However, they can be in linkage disequilibrium to the causal SNPs in a nearby region of NINJ2, such as in the promoter, the non-coding intronic site; and/or the open reading frame of the gene. NINJ2 is especially interesting due to its high degree of homology with adhesion molecules linked to anti-inflammatory response and tissue remodeling. NINJ2 also follows a functionally relevant neuronal/glial expression pattern following a sciatic nerve injury in rats (Milbrandt et al., 2000). This suggests that NINJ2 may contribute to the development, pathology, and/or recovery of a neurological disorder such as stroke.

NINJ2 has two transmembrane domains (green), two extracellular domains, and one cytoplasmic domain as shown in figure 3.1a. NINJ2 belongs to a family of proteins known as nerve injury induced proteins, or Ninjurins. The structural topology is characteristic of the protein members of the Ninjurin family. Ninjurins are cell adhesion membrane proteins that promote neuronal regeneration and have been suggested to mediate the recovery process of an injured nerve in the PNS (Araki et al., 1996; 1997). Cell adhesion molecules mediate cell-to-cell and cell-to-matrix interactions for the guidance of cells to a site of injury. There are two types of Ninjurins: NINJ1 in the mammalian genome (Milbrandt et al., 1996) and NINJA in *Drosophila melanogaster* (Zhang S. et al., 2006). NINJ2 shares conserved hydrophobic regions in the trans-

membrane domain with NINJ1 and NINJA and a high level of identical sequences with the extracellular domains of NINJ1 (Fig 3.1a).

NINJ1 mediates the heterophillic adhesion of leukocytes and vascular endothelial cells during vascular remodeling as well as a response to inflammation in the CNS. NINJ1 also enhances the apoptosis-inducing activity of leukocytes during tissue remodeling, suggesting NINJ1 is a major mediator of inflammation (Milbrandt et al., 2000; Lee H. et al., 2010). Fig 3.1B shows the adhesion motif in the sequence of NINJ1. NINJ2, however, does not share the same adhesion motif or mode of expression as NINJ1, suggesting it acts through a different mechanism underlying cell-to-cell interaction. Milbrandt et al. demonstrate that NINJ2 mediates homophillic adhesion of NINJ2 expressing cells. A peptide designed against an extracellular motif in the N-terminus domain of NINJ2 significantly decreases the adhesion capacity of NINJ2 expressing Jurkat cells (Milbrandt et al., 2000). Fig 3.1C shows the sequence that confers the largest adhesion capacity to NINJ2 expressing Jurkat cells as demonstrated in the adhesion experiments by Milbrandt. This sequence is highly conserved in NINJ1 and in NINJA.

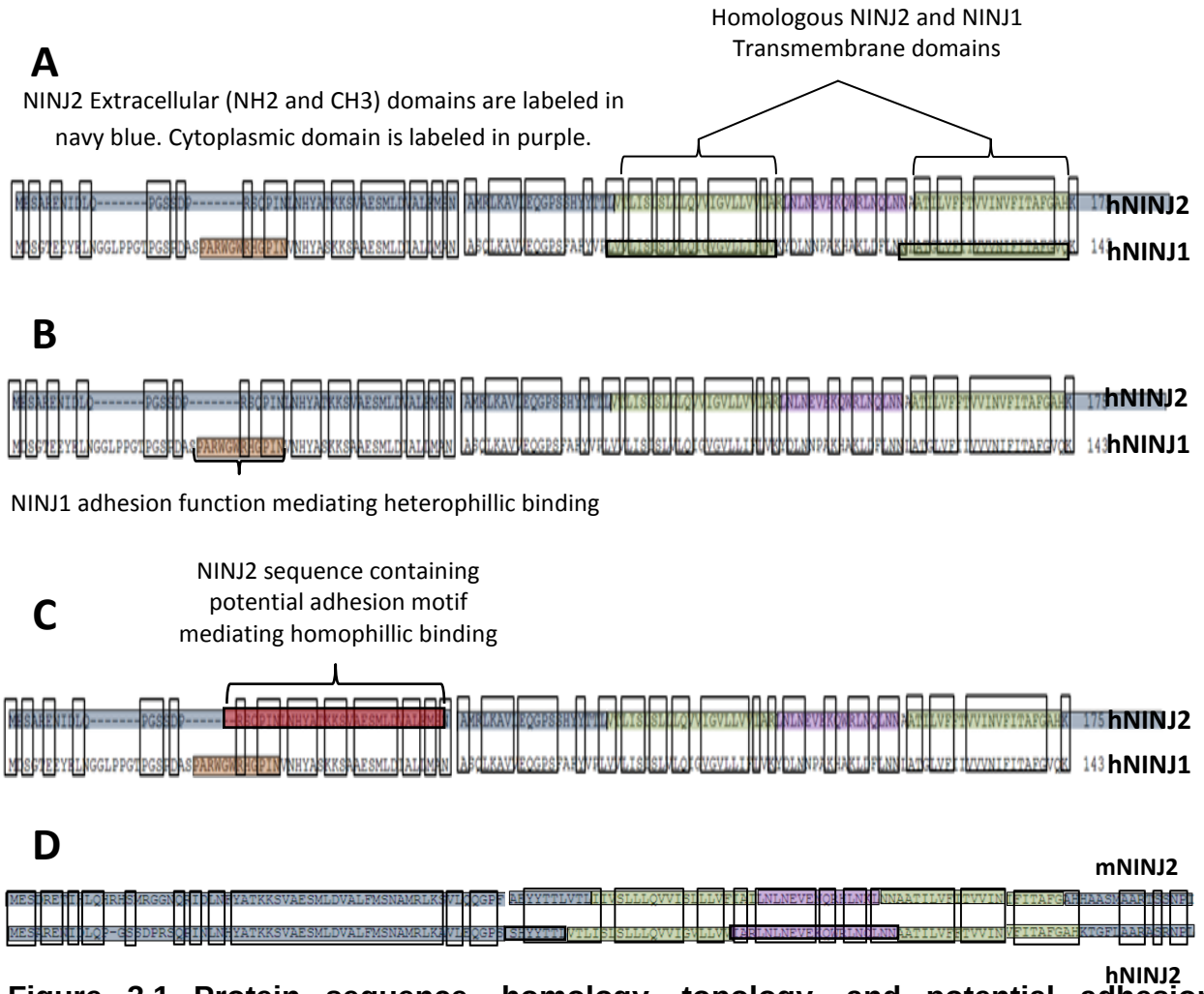

Figure 3.1 Protein sequence, homology, topology, and potential adhesion functions of NINJ2 and NINJ1. Transparent boxes demonstrate 100% identical sequences between the proteins. Figure 3.1 shows the hit of positive identical amino acid sequences between human NINJ2 and NINJ1 (52% identity) using the protein BLAST function (Altschul S. et al., 1997).

The sequence of NINJ2 with the highest homology to NINJA in *Drosophila* is shown in Figure 3.2 and it includes the proposed adhesion motif for NINJ2. NINJA mediates the adhesion of S2 cells and is essential for tissue remodeling of the tracheal system in *Drosophila*. This process is auto-regulated by the ENT domain of the same protein. First, the ENT domain of NINJA is cleaved by MMPs. Then, the ENT sequence signals the loss of adhesion of S2 cells and ends the process of tissue

remodeling (Zhang S. et al., 2006). Moreover, the same protein sequence as the one shown in Figure 3.2 also shows a similar pattern of homology with NINJ1 (Data not shown). The high degree of homology in the ENT domain in the three Ninjurins suggests that the adhesion motif of NINJ2 confers an important biological function.

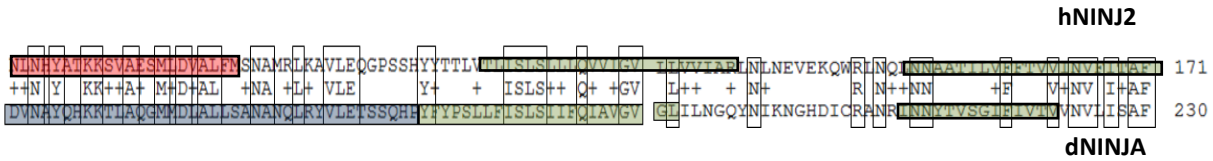

Figure 3.2 Protein sequence, homology, and topology of NINJ2 and NINJA. Figure 3.2 shows the sequences of human NINJ2 and *Drosophila* NINJA. It also shows the predicted intracellular domain (green bar) and 39 amino acids of the extracellular N-terminus (ENT) domain (blue bar) of NINJA and NINJ2. The intracellular domains are in a similar location. Most of the homology lies in the extracellular domain of NINJ2 and the extracellular region of NINJA as shown above.

Furthermore, NINJ2 is induced in Schwann cells one week after a sciatic nerve injury in the PNS of rats (Milbrandt et al., 2000). Schwann cells myelinate axons of motor and sensory neurons in the PNS. Schwann cells also aid in the regeneration of axons following axonal disintegration in the distal nerve stumps. This is evidenced by the retardation of axonal growth after the extraction of NMSCs cells in the distal stump of the peripheral nerve injury (PNI). Following an injury, Schwann cells dedifferentiate into immature Schwann cells that resemble the adult non-myelinating Schwann cells (NMSCs). NMSCs then proliferate and aid in the regeneration of injured axons (Fu S.Y. et al., 1997). This is of significance since the highest level of NINJ2 expression is seen in NMSCs and promyelinating Schwann cells distal to the site of injury (Milbrandt et al., 2000).

Schwann cells that myelinate large diameter axons develop into myelinating Schwann cells while those that myelinate small axons remain as NMSCs (Pereira J.,

2009). Following an injury, Immature Schwann cells interact promiscuously with many axons but eventually turn into promyelinating Schwann cells. Promyelinating Schwann cells wrap around one axon at a time. This process is mediated by the epidermal growth factor receptor-Neuregulin 1 (ErbB-NRG1) signaling pathway (Raphael AR. et al., 2011). Myelination by Schwann cells facilitates faster conduction velocities in axons (JEssen K. et al., 2010), induces mitochondrial activity in myelinated axons (Zambonin J. et al., 2011), and stabilizes the point-to point connectivity during the branching process of developing neurons (Griffin JW et al., 2008).

NINJ2 also seems to mediate the adhesion of NMSCs to unmyelinated nerve fibers (Milbrandt et al., 2000). After an injury, NMSCs position themselves closer to the cell bodies of unmyelinated nerve fibers with the aid of adhesion molecules. Once NMSCs are stabilized in the area of injury, they extend their processes onto unmyelinated fibers and signal other denervated glial cells to adhere onto these cells. This aids in the regeneration of damaged nerves through the differentiation of NMSCs into myelinating Schwann cells (Griffin JW et al., 2008 and Joung et al., 2010). Unmyelinated axons of small diameter, including C fibers nociceptors, instead, wrap inside invaginations formed by NMSCs, also known as Remak bundles (Murinson BB et al., 2005). These fibers retain a higher degree of plasticity and a larger capacity to sprout collaterally throughout these processes of regeneration (Vlader A. et al., 2011). NINJ2 is not known to be expressed specifically in Remak bundles. However, given that the highest level of induction of NINJ2 is distal from the site of injury (Milbrand et al., 2000), it is suggested that its induction in NMSCs is crucial for the regeneration of peripheral unmyelinated nerves in Remak bundles. Furthermore, the role of NINJ2

expression in the CNS is not well understood. The gene expression of NINJ2 is lower in human and rat brains than in other tissues, such as in the bone marrow, as indicated in figure 3.3 (NCBI's Unigene dataset) and Milbrandt et al., 2000, respectively. For instance, NINJ2 is expressed at a relatively lower level in normal brain samples than in the lung.

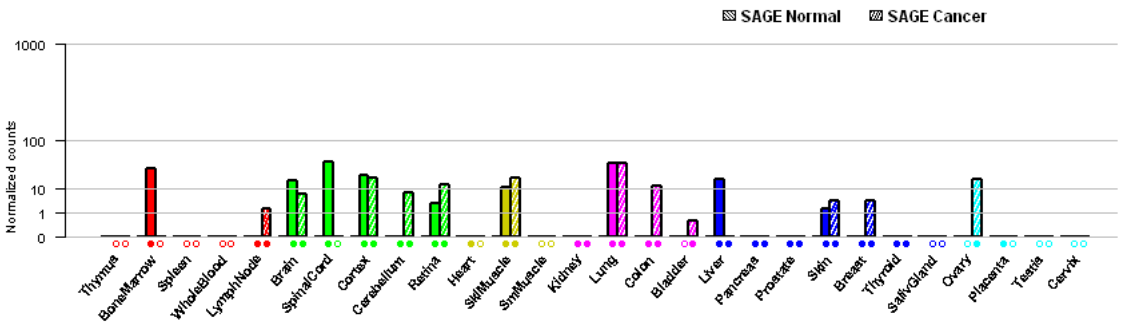

Figure 3.3 Expression level of human NINJ2 from Northern blot data across normal and cancer human tissues (CGAP datasets from *Hs.frequencies* and *Hs.libraries*). Data show the ratio of "the number of appearances of SAGE [NINJ2] tags divided by the total number of tags in that particular tissue" normalized by 1.2 M (www.genecards.org/info.shtml#expression_images).

NINJ2 has also been shown to be expressed in the radial glia, also known Bergmann cells, in the developing brain (Milbrandt et al., 2000). This suggests NINJ2 may play a role in a similar regenerative phase following an injury in the CNS. This is evidenced by the relatively high level of expression of NINJ2 in the spinal cord and the induction of neurite extension from tissue cultures of the dorsal root ganglion (DRG) by NINJ2 expressing cells *in vitro* (Milbrandt et al., 2000). NINJ2 may affect how the sensory system in the PNS responds to an injury in the CNS following a stroke. A deficiency in the function of the sensory system in the PNS, for instance, is characteristic of loss of sensibility in stroke patients. Moreover, there is a higher

coverage of Schwann cells onto efferent spinal cord fibers than on afferent fibers from the DRG (Murinson and Griffin, 2004). Thus, a deficiency in the adhesion of Schwann cells to unmyelinated nerve fibers may lead to the reduction of the sensory capability of efferent unmyelinated fibers (Vlader A. et al., 2011). This may result from a reduction in the expression of molecules like NINJ2 at acute phase of injury (Milbrandt et al., 2000). Further research is needed on the molecules that mediate the transition from neural degeneration to recovery.

\

EXPERIMENTAL RATIONALE

This study uses an induced mouse model of a Middle Cerebral Artery occlusion (MCAo) in order to determine the changes in expression of NINJ2 after a stroke in mice brains. The mouse sequence of NINJ2 (mNIN2) is 73% identical to the human sequence of NINJ2 (hNINJ2) as shown in figure 3.1D. The tissues taken for analysis include cortical tissue with the focal lesion of stroke as well as the surrounding penumbra. Experimental samples include RNA and tissue lysates from cortical tissues of ipsilateral brain hemispheres of the MCAo induced mice. The internal controls for qPCR include cortical tissues from three healthy mice brains. Tissues are extracted from stroke induced mice 3 hours, 24 hours, 3 days, 1 week, and 2 weeks following reperfusion. This timeline is representative of the injury and recovery stages following the stroke.

Research aims and hypothesis

Aim 1: Quantify changes in gene expression of NINJ2 after a stroke.

AIM 2: Quantify changes in protein levels of NINJ2 after a stroke

Hypothesis: <u>Gene and protein expression of NINJ2 changes as a result of stroke.</u>

RESULTS

Calculation of the Amplification Efficiency as a measure of probe sensitivity TaqMan assays. In order to determine the sensitivity of the TaqMan qPCR assays, relative quantification (RQ) of NINJ2 expression was measured by the comparative Ct ($2^{-\bullet C'_T}$) method. This method presumes that the amplicon specific amplification efficiencies of the qPCR assays are calculated *a priori*. The amplification efficiencies (E) and percent efficiencies (%E) are calculated using Equations 1 and 2 in the methods section (Rasmussen, R. 2001). QPCR amplification efficiency is tested by performing a serial dilution of cDNA templates extracted from naïve cortical brain samples. Each sample is tested in triplicate. The details of the testing results for each qPCR experiment are shown in Table A1 in the appendix. Each of our qPCR experiments allows for a maximum of three serial dilution points. An efficiency value of 2 also indicates strong probe sensitivity for the target sequence at the range of the input cDNA concentrations (1000ng to 0.1ng). The probe efficiency and sensitivity is also tested and verified by performing four independent serial dilution experiments with eight (first two reactions) and four (second two reactions) serial dilution points using the same cDNA template stock. The slope of the dilution curve is determined by plotting Ct values as a function of the log of the cDNA input concentration values.

The qPCR amplification efficiency results for the NINJ2 and RPOL2 probes are shown in Figure 3.3. Figure 3.3 demonstrates that the NINJ2 and RPOL2 probes are sensitive up to approximately 36 and 34 cycles of PCR amplification, suggesting accurate C_T values at a wide dynamic range of input cDNA concentration. The assay efficiencies are assessed by the slopes of the standard dilution curves, as indicated in

figure 3.3. The efficiencies are 1.93 and 1.98 for NINJ2 and 1.96 and 1.99 for RPOL2. The % efficiencies are 92.7% and 98.1% for NINJ2 and 96.3% and 98.6% for RPOL2. The efficiencies of both assays are within 10% difference from each other. This demonstrates their performance in the qPCR reactions and permits the implementation of the $2^{-\bullet\bullet}$ $_{T}$ method for the relative quantification analysis. The amplification results for INOS2 are shown Figure A.3 in the appendix. The slopes of the standard dilution curves for the two NINJ2 assays are -3.5 and -3.4. The slopes of the standard dilution curves for the two corresponding RPOL2 assays are -3.41, and -3.36. The correlations observed between the log amount and resultant C_T values for each probe assay are strong. All of the regression coefficients (R^2 values) are greater than 0.99.

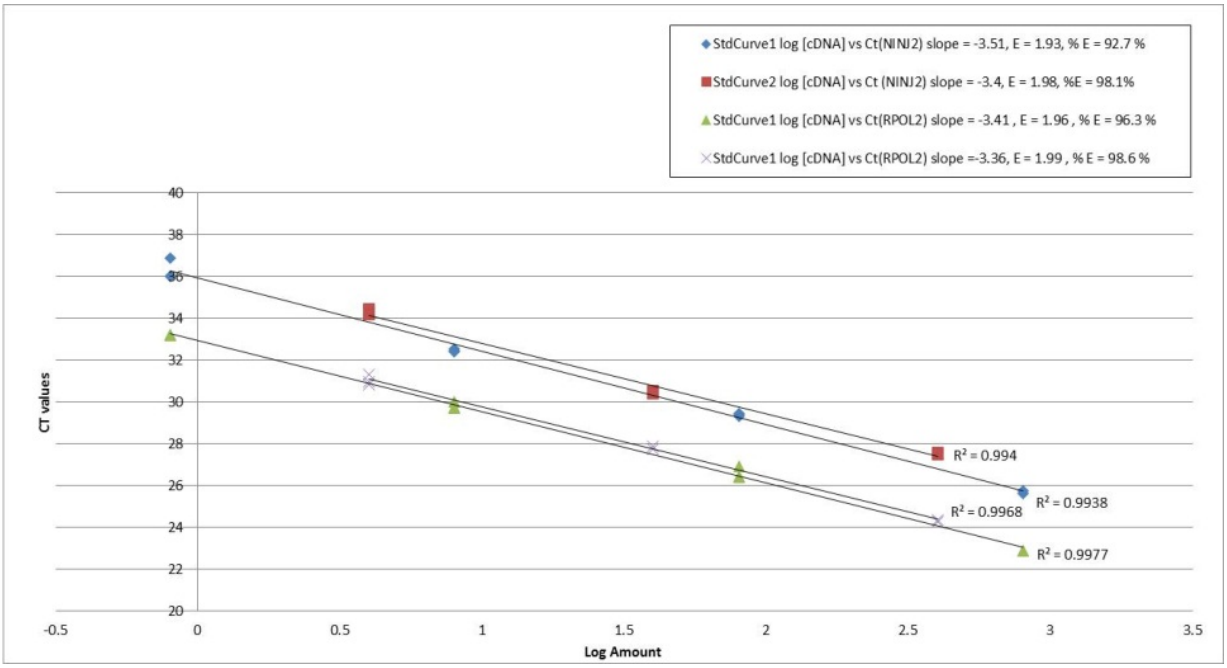

Figure 3.3 Determination of QPCR efficiencies of target gene (NINJ2) and reference gene (RPOL2). Ct values (y-axis) versus the log of cDNA concentration (x-axis) are plotted in order to calculate the slope. Each standard curve represents an independent experiment.

Timeline of Expression of NINJ2 in cortical tissues of MCAo Stroke induced mice brains and validation of results by the expression profile of INOS-2.

Increasing NINJ2 gene expression 7 days after stroke in the ipsilateral cortical tissues of MCAo mice brains. In order to determine changes in the gene expression of NINJ2 and INOS2 due to an induced MCA occlusion in mice, three primary ischemic (ipsilateral) cortical tissues and three matched control (contralateral) cortical tissues are evaluated at five time-points (3hours, 24hours, 3days, 7days, and 14days) after reperfusion. cDNA is pre-amplified and tested for relative changes in the mRNA levels of NINJ2 and INOS-2 using the comparative Ct method. RQ values are normalized to changes in the expression of RPOL-2 housekeeping gene and compared with the expression of NINJ2 in cortical tissues of healthy mice brains. Figure 3.4 demonstrates changes in the induction of NINJ2 in the ipsilateral and in the contralateral cortex. The details of the calculations and test results are shown in figure A.6 in the appendix. There is no significant change in NINJ2 gene expression in the contralateral cortical tissue at any time point although there is a slight decrease in expression at 24hr after stroke, which did not reach statistical significance (P=0.06). In the ipsilateral cortical tissues, there was a significant induction in NINJ2 expression at 7 days (2.2 fold; P=0.007), which is slightly attenuated at 14 days (1.9 fold; P=0.07).

Figure 3.4 Pattern of expression of NINJ2 in the ipsilateral and contralateral cortical tissues of MCAo brains compared with expression in healthy mice brains (naïve). The red asterisk indicates a significant fold induction (*2*-

Increasing expression of INOS2 3_days and 7 days after stroke and maximum induction of expression at 3_days after stroke. In order to validate changes in the expression profile of genes induced after a stroke, we also study changes in the expression profile of an inducible gene (INOS-2) that is up-regulated as a result of post-inflammatory processes from a stroke. Figure 3.5 demonstrates changes in the fold induction of INOS2 in the ipsilateral cortex. The details of the calculations and test results are shown in figure A.6 in the appendix. There is no significant change in INOS2 gene expression in the contralateral cortical tissue at any time point. In the ipsilateral cortical tissues, there is a significant induction in INOS2 expression at 3 days (3.5 fold; P = 0.05) and 7 days (2.2 fold; P=0.05).

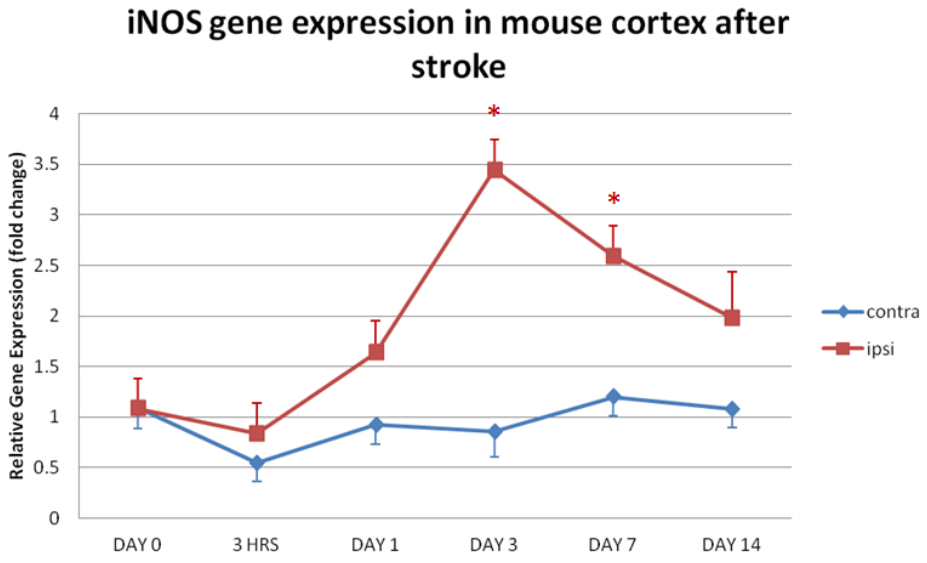

* P<0.05

Figure 3.5 Pattern of expression of INOS2 in the ipsilateral and contralateral cortical tissues of MCAo brains. The red asterisk indicates a significant fold induction (*2-• C'T*) of INOS2 in the ipsilateral tissues. The blue number sign indicates a significant fold induction of INOS2 in the contralateral tissues. The data points for the time-point results show the average of RQ compared to the naïve samples from the same qPCR experiments.

Characterization of the specificity of an anti-human NINJ2 antibody for the study of changes in the levels of NINJ2 protein molecules in cortical tissues of mice brains after stroke.

Selectivity of the a-NINJ2 Antibody in detecting the 23 KD band in the mouse brain, lung, and 293+NINJ2 cell lysates. In order to detect changes in the levels of the protein molecules of NINJ2 after stroke, it is necessary to acquire an antibody that detects NINJ2 in the mouse brain and in positive controls that over-express the NINJ2 gene. The molecular size of NINJ2 (23KD) is originally reported in over-expressing Chinese Hamster Ovary (CHO) cells by Milbrandt et al., 2000. The positive controls consist of protein lysates from mouse lung tissue and NINJ2 over-expressing 293-T cells. In figure 3.7, we report the detection of the molecular size of NINJ2 (23 KD) in 80 µg of mouse brain and 30 µg of lung tissue lysate as well as in cell lysate of NINJ2 over-expressing 293-T cells by a commercially available antibody from Protein Tech Inc. It shows the detection of a protein signal at 23KD in both the whole homogenate and supernatant fractions of the brain and lung tissues. The antibody detects higher levels of protein in the whole tissue homogenate than in the supernatant fraction of the lung tissue. The whole tissue homogenate lysate carries a high concentration of membrane proteins, thus improving the chance for its detection of the membrane NINJ2 protein. The results also demonstrate the presence of the 20 KD and 16 KD bands in the lane using the 293+NINJ2 cell lysate.

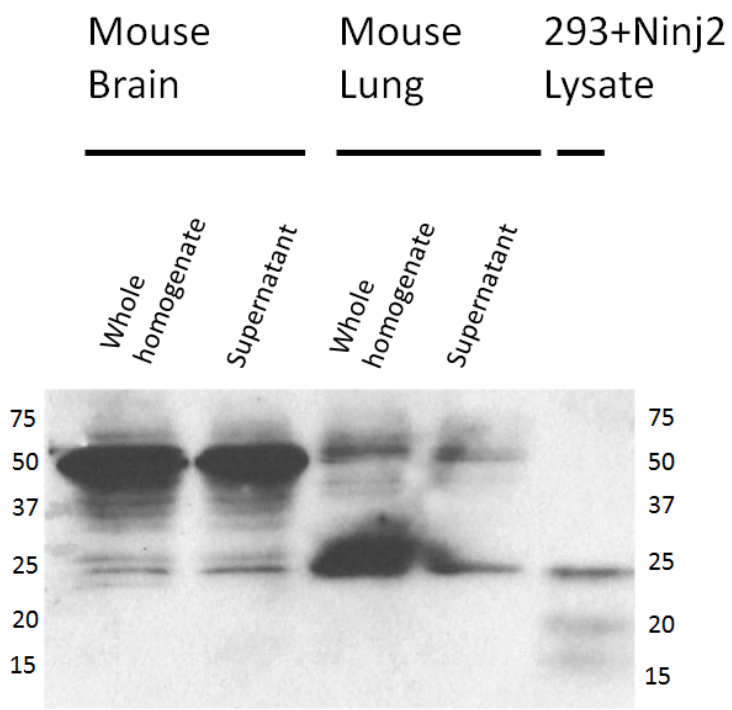

Figure 3.6: Detection of mouse brain and lung proteins with a molecular size of 23 KD by the Protein Tech a-NINJ2 Ab. Samples include mouse brain (first two lanes), mouse lung (lanes 3 and 4), and human 293-T cells transfected with human NINJ2 cDNA.

Specificity of the P. Tech antibody in detecting the NINJ2 protein at 23KD in the mouse brain cortex. In order to assess the specificity of the antibody to recognize the proteins of NINJ2 at 23KD in cortical brain tissues and 293+NINJ2 transfected cell lysates, a peptide competition and an immunoprecipitation assay are performed. The purpose of these experiments is to reduce the possibility of obtaining a false positive result at 23KD. The experimental lane is run alongside the negative control lane and a protein ladder in the gel. The reduction in the signal of a band in the experimental lane compared to the control lane is indicative of the selectivity of the antibody against the target protein. Figure 3.7 uses protein lysate from brain, lung, and transfected cell lysate and it shows significant reduction in the protein level at the 23KD band from the lung and 293+ lysate. Figure 3.7a shows the disappearance of the 23 KD band in the mouse brain tissue after 200X molar peptide incubation with the P. Tech antibody for 1 hour at room temperature. Figure 3.7 b shows a slight reduction in the band intensity of the brain while figures 3.7 (c and d) show a significant reduction in the band intensity of the lung and 293+NINJ2 lysates after antibody-peptide incubate overnight at four degrees Celcius. This suggests that the temperature changes the conformation of the NINJ2 antigenic site in the antibody, and thus prevents it being exposed to the peptide, as when it is performed at room temperature. This figure suggest for the competition of the antigen binding site in the NINJ2 antibody.

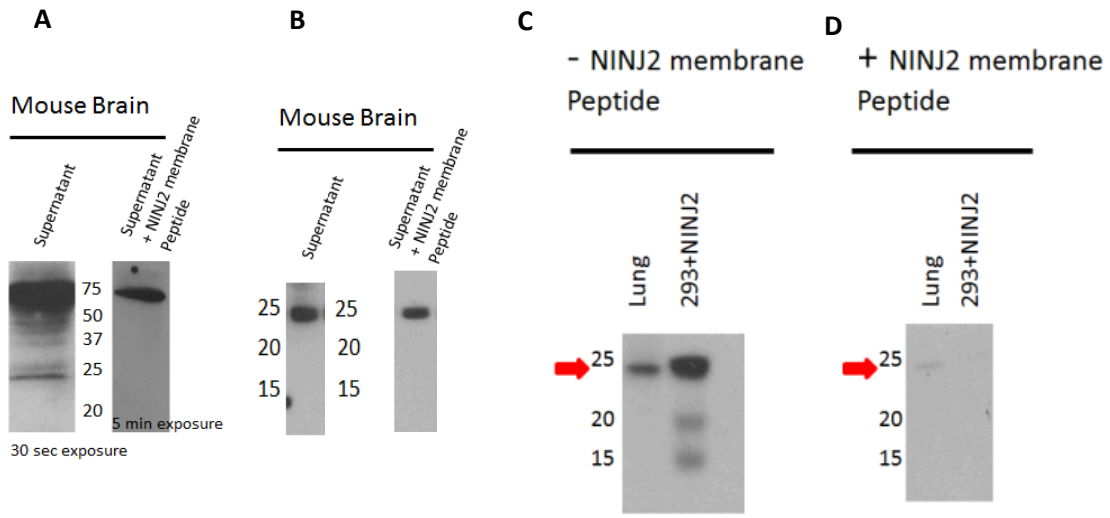

Figure 3.7: **Results from the peptide competition experiment using mouse cortical brain tissue (A AND B), lung and 293+NINJ2 transfected cell lysates (B AND C).** Commercially acquired peptides (Santa Cruz sc-79653) mapping membrane domain of the NINJ2 protein sequence is used to compete for the antigenic site of the P. Tech a-NINJ2 antibody. The peptide competition experiments are performed using protein lysate from the mouse brain and lung tissues and 293+ NINJ2 transfected cells.

Validation of the specific nature of the antibody by its ability to immuno-precipitate the NINJ2 protein at the 23KD band. In order to verify the immunogenicity of the P. Tech antibody to the whole sequence of the NINJ2 protein at 23 KD, we tested the ability of the antibody to immuno-precipitate (IP) the NINJ2 antigen from the mouse brain and 293+NINJ2 transfected lysates. The P. Tech antibody is tested for its specificity to detect the NINJ2 antigens in the protein lysate solution. The immunoprecipitation assay consisted in incubating the antibody molecules-bound to magnetic beads coated with protein G- with protein lysates. For every IP experiment, a negative IgG antibody raised in rabbits is used in order to differentiate the background bands from the specific band detected by the a-NINJ2 antibody. A low stringent solution is then used to separate the antigens from the antibody and preserve the structural conformation of the protein as much as possible. We use silver staining of the antigens isolated from the protein lysates to validate the specificity of the antibody. Figure 3.8 shows silver staining of a protein gel loaded with the precipitated sample from the experimental and the negative IgG control lane. It also shows the isolation of the 23 KD band, along with other non-specific bands at higher molecular sizes. Figure 3.9 also detects the precipitation of the 23 KD band in the experimental lane of the membrane blots from the 293+NINJ2 and brain lysate solutions. The results in the first lane of each blot in figure 3.9 indicate a detection of different protein sizes, including a molecular size at 23 KD corresponding to the band of the NINJ2 protein. The control IgG is also immunoreactive to proteins at the same molecular size although at much lower levels. It also shows two other bands at 31KD and 38KD. Both results suggest that the P. Tech antibody selects for the NINJ2 protein

at 23KD out of all the other non-specific protein bands in the brain tissue lysate and the positive 293+NINJ2 control.

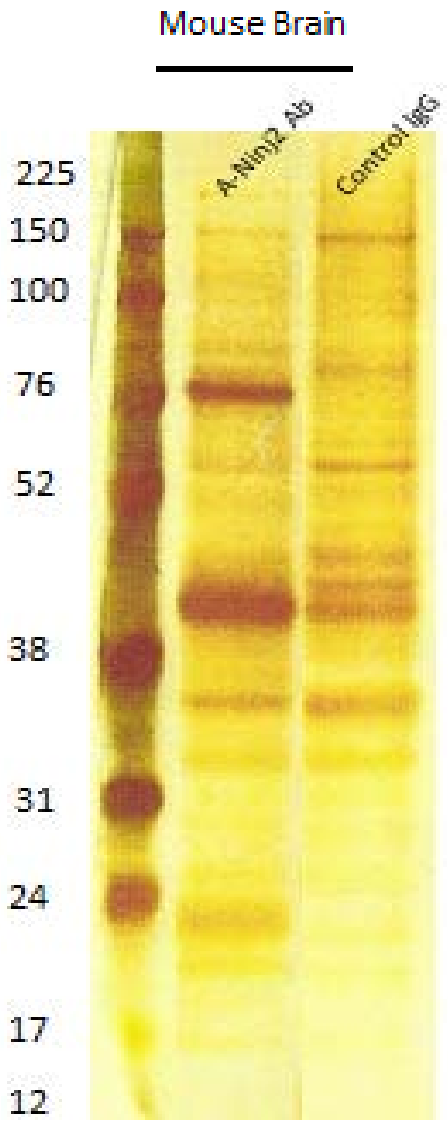

Figure 3.8: Silver staining of the immuno-purified antigens from the immunoprecipitation experiment with the mouse brain tissue. In the first lane, the P. Tech NINJ2 antibody is used to purify the NINJ2 antigen from the brain sample. In the second lane, the IgG control is used to validate the reactivity of the P. Tech antibody to NINJ2 in the brain sample. The IgG control is obtained from the same species (rabbit) where the P. Tech antibody is raised in. The silver staining is performed on a protein gel that carries the immuno-purified brain sample concentrated with the NINJ2 antigen.

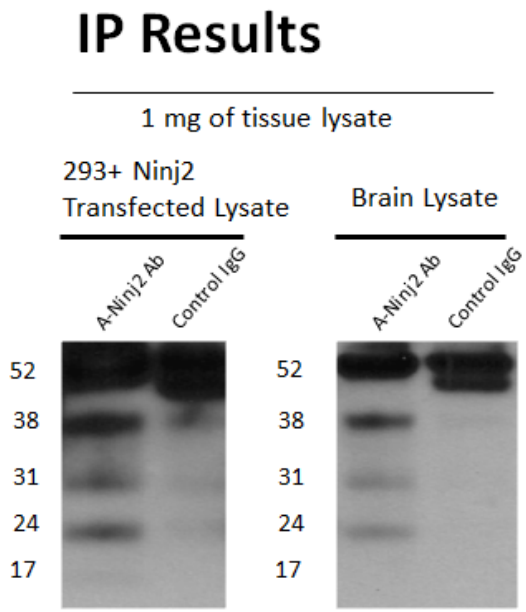

Figure 3.9: Detection of the 23KD band by immunoprecipitation of the NINJ2 molecules from protein lysates of the 293+NINJ2 transfected cells and mouse brain samples. The antigen is purified using the P. Tech Antibody as described in the methods section for IP. The first lanes of each blot represent the purified NINJ2 antigen from the 293+ transfected lysate and the brain lysate samples. The second lanes of each blot represent the control IgG used in the IP experiments.

Increasing protein levels in the contralateral and ipsilateral cortical tissues at 7 and 14 days after stroke.

In order to assess changes in the protein expression of NINJ2 due to an induced MCA occlusion in mice, three primary ischemic (ipsilateral) cortical tissues and three matched control (contralateral) cortical tissues are evaluated at three time-points (24hours, 7days, and 14days) after reperfusion. Tissues are homogenized in tissue lysate (1X RIPA) solution to test for changes in the protein levels of NINJ2 with western blotting. The relative densities of light intensities (RD values) of the protein bands detected at 23KD by the P. Tech antibody are normalized to changes in the RD values of the protein standards. The standards consist of B-Actin bands at 42 KD (as shown in the second rows of the immuno-blots in fig3.10). The resultant values are reported as normalized relative densities (NRD) and are compared against the NRD values of the cortical tissues of a naïve mouse brain. Figure 3.10 indicates an increase in the protein levels of NINJ2 in the ipsilateral brain cortex 7 days (4.5 fold) and 14 days (4 fold) after a stroke. It also shows an induction in the protein levels of NINJ2 in the contralateral tissues 7 days (6.5 fold) and 14 days (4 fold) after stroke. Because of the low number of animals for which results are obtained, it is chosen present averages without standard deviations.

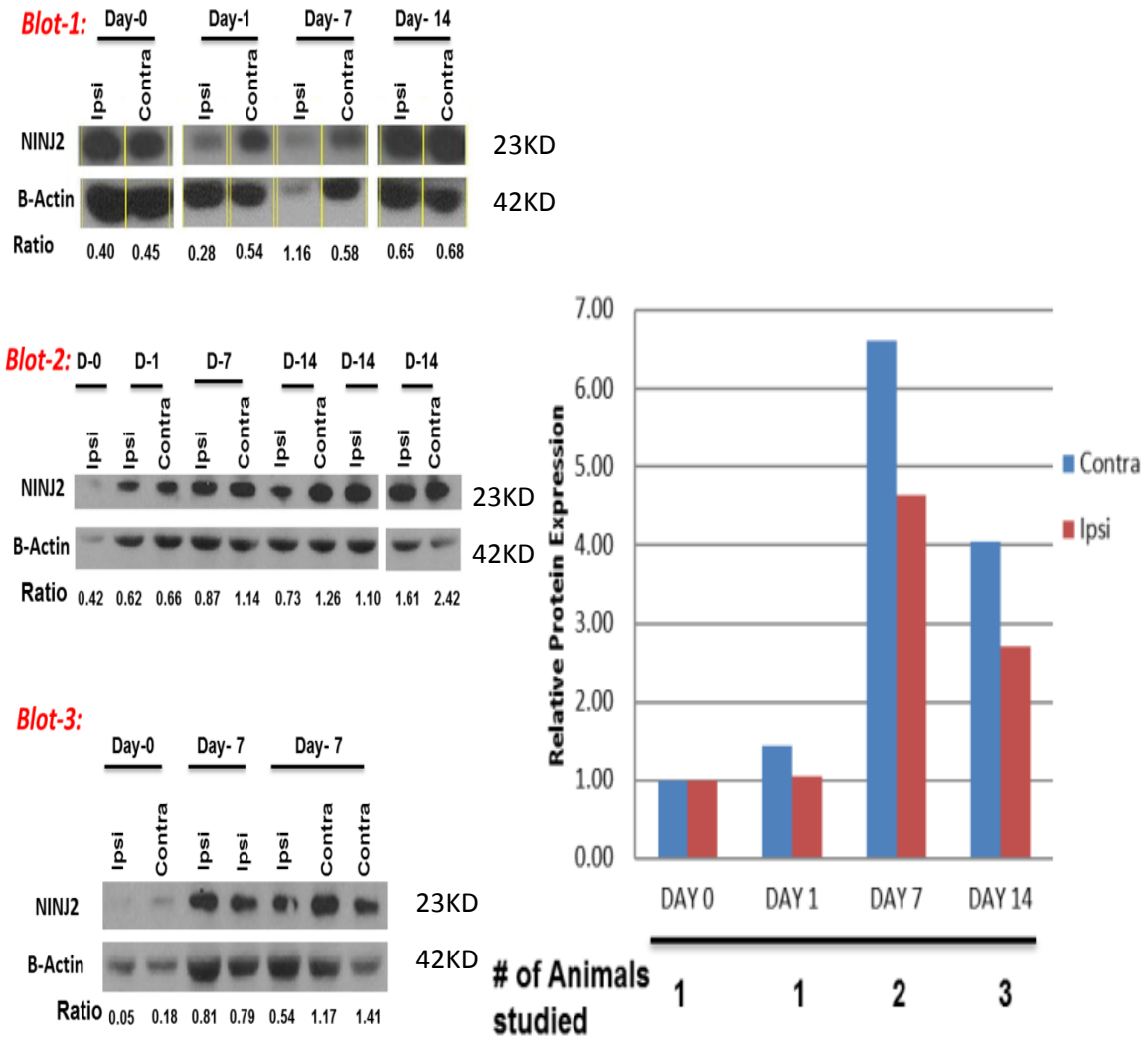

Figure 3.10: Changes in the protein levels of NINJ2 in mice brains following a stroke. The results show an increase in the levels of the 23KD band corresponding to changes in the NINJ2 protein levels in the ipsilateral cortical tissues of mice brains 7days and 14 days after stroke. It also shows an increase in NRD values of NINJ2 protein expression in the contralateral cortical tissues 7days and 14days after stroke. These results are produced from the tabulation of the normalized relative density ratios obtained in the western blot procedures. The results indicate a higher induction of protein expression in the contralateral than in the ipsilateral cortical tissues tissues.

DISCUSSION

A Genome-wide Association Study (GWAS) from four large prospective cohorts in the USA and Europe identified an association of two Single Nucleotide Polymorphisms (SNPs) on chromosome 12p13 with a greater risk of ischemic stroke in individuals of European and African-American ancestry. This generated a hypothesis regarding a potential candidate gene for stroke. The GWAS reports data on the association of SNPs to greater susceptibility of stroke. The GWAS-detected SNPs are located 11 Kb upstream of the Ninjurin 2 (NINJ2) gene. Many weakly associated SNPs are located within the coding and promoter regions of NINJ2 (Ikram *et al.,* 2010). This has led us to hypothesize that the causal SNP for stroke may be related to NINJ2 function. If the causal SNP is located in a regulatory and/or a functional region of NINJ2, it may result in the alteration of the expression and/or function of the gene. This change may alter the susceptibility for the disease and/or worsen the progression of the disease. The SNP is associated with a greater susceptibility to incidence of stroke. Changes in expression are evaluated following a time-course of five time-points (3hours, 24hours, 3days, 7days, and 14days) after reperfusion. Data suggest a 2.3-fold induction in NINJ2 gene expression in the ischemic core and the peri-infarct tissue to the ischemia (Ipsilateral) cortex at 7 days after stroke, which persists at 14 days.

In order to clarify the possible role of NINJ2 in stroke, we sought to determine whether there will be changes in the expression levels of NINJ2 in the ischemic brain cortex of a transiently induced mouse that models a focal Ischemic stroke in humans. This model permits the record of behavioral as well as biochemical changes as mice

progress from acute to the recovery stages of stroke. Changes in expression of NINJ2 are reported following a stroke.

GWAS discovered a SNP with greater risk to a clinically recognized onset of stroke. Our results demonstrate changes in expression of NINJ2 following a stroke. The induction of expression of NINJ2 at 7 days suggests NINJ2 plays a role as a molecular mediator of recovery. However, further functional experiments are needed, i.e. knocking out NINJ2 in the mouse and inducing it with stroke, in order to establish the role of NINJ2 in the recovery phase of stroke. Our results suggest that expression of NINJ2 in the cortex may be associated with a delayed onset of stroke. Therefore, it is necessary to determine an association between the frequencies of SNP with the time of onset of stroke. Furthermore, the GWAS does not take into account clinically unrecognized mini-strokes that may occur over the life-time of an individual. Based on our results, if the gene plays a role as an endogenous recovery mediator of stroke, individuals over-expressing the gene after a mini-stroke may be less susceptible to an early onset of a bigger stroke. NINJ2 may also be transcriptionally suppressed in people with greater susceptibility to an early onset of stroke. It will also be of interest to perform a GWAS between the SNPs and the expression of NINJ2 in people with time of onset of stroke. This may determine a functional interaction between NINJ2 and other genes involved in susceptibility to delayed onset of stroke. Also, it is hypothesized that attenuation in the expression of the gene may result in less protection from cortical damage by the stroke. Those with an over-expression of the gene may be protected from damage to the cortical tissue as a result of stroke. Thus, attenuation in the

expression of NINJ2 may be indicative of greater susceptibility to a greater damage from the stroke.

A potential contribution of NINJ2 to stroke can be deduced from the biological pathway of genes with similar gene expression profiles as NINJ2 (Hughes T.R. et al., 2000). The temporal expression profile of NINJ2 is similar to the pattern of expression of NINJ2 and NINJ1 following a transected and crush sciatic nerve axotomy. The pattern of expression of NINJ1 following a sciatic nerve axotomy shows that it is up-regulated beginning at 16 hrs after injury (Araki et al., 1996). Data for NINJ2 in the same model shows that it is up-regulated beginning at 7 days after injury. Both in NINJ1 and NINJ2 level of expression reaches peak levels 7-14 days after the injury and remain elevated for up to 56 days after injury (Milbrandt et al., 2000). The induction of expression of the Ninjurin genes occurs in the segment distal to the injury after either transection or crushed. NINJ1 mediates leukocytes recruitment in the cerebral vasculature after inflammation. This response to inflammation is also known to take place at the acute phase of stroke (Lee, Hyo-Jong et al., 2010). Since the gene expression of NINJ2 is not significantly altered at this stage, NINJ2 may not be involved in this humoral process of inflammation. NINJ2 also doesn't share same adhesion motif as with NINJ1. However, both NINJ1 and NINJ2 facilitate the neurite outgrowth from peripheral motor neurons. This suggests that NINJ2 is active and performs the same function as NINJ1 at later time-points following injury. This may be a reason why NINJ2 may not be involved in the humoral response in the acute phase of stroke (Lee, Hyo-Jong et al., 2010). Our data supports the notion that NINJ2 is relevant to recovery mechanisms distal to an area of stroke.

NINJ2 is also induced in Schwann cells at the late stages of recovery from a nerve injury in rats. Schwann cells are glial cells that over-express NINJ2 at the early stage of maturation and those with no myelination capacity. These cells support neural regeneration from an injury in the PNS by adhering to and facilitating conductivity in neurons, suggesting NINJ2 plays some role in the repair of nerve damage. NINJ2 is also found to be constitutively expressed at low levels in radial glia in the CNS (Milbrandt et al., 2000). This indicates that NINJ2 is expressed in cells at early stages of maturation and may play a role in the cellular response to a disease.

The gene pattern of expression of NINJ2 is also similar to the pattern of expression of the nerve growth factor (L1) and neural cell adhesion molecule (N-CAM) after injury. These adhesion molecules facilitate the cell-to-cell interactions between Schwann cells and neuronal axons following a sciatic nerve injury in the PNS. The expression of L1 and N-CAM is induced in non-myelinating Schwann cells one week after the injury. The time course of expression following sciatic nerve injury is similar to that of NINJ1, neural CAM, and L1 following a transected sciatic nerve axotomy. Adhesion molecules such as MCAM or L1 also enhance neurite outgrowth in the same manner as NINJ1 and NINJ2 (Milbrandt et al., 2000). Given this pattern of expression, NINJ2 protein may be classified as molecule involved in the recovery process of nerve regeneration in the peripheral nervous system as well as in the central nervous system after stroke.

Data also suggest an increase in the protein levels of NINJ2 in the Ipsilateral and contralateral tissues at 7 days, which also persists at 14 days. The significant injury-induced induction of the mRNA and protein levels occurs at 7 days. Furthermore,

there seems to be a larger production of the NINJ2 protein in the contralateral compared to the ipsilateral cortical tissues. This is not consistent with the gene expression results since mRNA levels do not show a significant change in the contralateral tissues. Data from peptide competition and immunoprecipitation assays seem to suggest that the 23 KD band corresponds to the NINJ2 protein. As suggested from the peptide competition results, the antibody binding site of the Protein Tech antibody is competed against a peptide mapping within the membrane domain of the mouse NINJ2 sequence. Data indicate a very slight decrease in the light intensity of the band at 23 KD in brain in the presence of the peptide when exposed at $4^{o}C$ (fig 3.7b). This suggests that the binding site of the antibody does not confer a high degree of affinity to the epitope mapping a membrane region of NINJ2, assuming equal loading. The evidence that results obtained from antibody-peptide incubation at $4^{o}C$ is not due to chance, is the significantly higher competition with NINJ2 that is shown in the lung and transfected lysates (figs. 3.7c and d). A possible reason for the inconsistency in the peptide competition results with NINJ2 antigens in the brain, lung, and transfected lysates may be due to the low expression of the protein in the brain. The sample in the brain tissue lysate would expose less amount of the NINJ2 protein for the antibody-peptide interaction. The immunoprecipitation assay also provides an indirect evidence for the identification of the NINJ2 protein at 23 KD, as suggested by Figure 3.8.

A limitation of the antibody characterization study is that we have no direct proof that the 23 KD band corresponds only to the NINJ2 molecule. For instance, the immunoprecipitation study only offers indirect evidence suggesting that the Protein Tech antibody detects NINJ2 at 23KD but it does not rule out the possibility of it also

detecting an identical protein such as NINJ1. It may be that the Protein Tech antibody is detecting both NINJ2 and NINJ1 proteins in the samples. In fact, Araki et al. report the molecular weight of NINJ1 also to be at 22 KD. Thus, it may be that the a-human NINJ2 antibody from Protein Tech also detects the mouse form of NINJ1 (Araki et al., 1997). This antibody may be recognizing epitopes specific in NINJ2 as well as in the NINJ1 proteins in the membranes.

A temperature of 4 ^{o}C is maintained for all the incubation steps with the Protein Tech antibody throughout the experiments. These include the protein transfer and membrane incubation steps in the western blot experiment; the peptide incubation step in the peptide competition assay; and the brain tissue lysate incubation in the immunoprecipitation experiment. The cold temperature may be maintaining the non-linear structural conformation of the NINJ2 protein, thus exposing the structural epitopes for their detection by the Protein Tech antibody. However, this conformation may also be preserved for other homologous proteins, such as NINJ1. The antibody from Protein Tech is raised against the whole recombinant protein of NINJ2, thus increasing the likelihood of detecting small differences in structural conformation in the proteins. Consequently, this may induce the cross-reactivity by the Protein Tech antibody with NINJ2 and NINJ1. Another reason why the antibody may be detecting NINJ1 in the samples is that the pattern of expression of NINJ1 at 7 days after sciatic nerve injury is similar to that of NINJ2 (Araki et al., 1997).

If the pattern of expression of the 23 KD band corresponds only to changes in the NINJ2 protein, then it is suggested that the NINJ2 protein levels are increased as part of an unknown recovery mechanism from stroke. For instance, NINJ2 may mediate the

adherence of molecules in the induction of anti-inflammatory processes in the brain. This suggests for a global increase of protein expression of NINJ2 in the brain cortex 1 week after stroke. The gene expression is up-regulated in the ipsilateral cortex while the protein levels increase in the contralateral cortex 7 days after stroke. The gene expression of NINJ2 is un-regulated in the contralateral cortex. It may be that post-transcriptional event down-regulates the expression of NINJ2 in the contralateral tissue. This would seem to suggest that once the NINJ2 protein molecules are produced in the penumbra, these then trans-locate from the injured cortex to the healthy hemisphere, where it maintains an induced level at the late recovery stages following stroke.

Moreover, the protein levels of NINJ2 may be significantly higher in the contralateral cortex after stroke where synaptic plasticity is known to occur. Thus, NINJ2 may have additional synergistic effect on synaptic plasticity in the contralateral cortical tissue of the brain after stroke. In order to assess the significance of changes protein levels at this time-point, it is necessary to include more mice in the experiments. However, it is not possible to conclude about the biological significance of changes in the protein levels as a result to stroke. This is due to one of the major limitations of our study, the fact that we don't have an antibody that is only specific for the mouse NINJ2 protein.

CONCLUSION

A GWAS study has found two SNPs associated with greater susceptibility to incidence of ischemic stroke in the general population. These SNPs, located upstream of the NINJ2 gene, are not necessarily the causal variants of the disease. If the causal SNP is located in a regulatory and/or a functional region of NINJ2, it may result in the alteration of the expression and/or function of the gene. We have characterized the pattern of expression of NINJ2 in the brains of MCAo induced mice models at different time points following a stroke. The NINJ2 pattern of expression suggests that it may be induced at the late-time phases after stroke. Although a larger number of animals are needed at 1week and 2weeks time-points, our results are consistent with experiments that demonstrate a similar pattern of expression following sciatic nerve injury in the peripheral nervous system. Therefore, it is hypothesized that any change in the expression of the gene that may be induced by the causal SNP in the population may be of significance for the recovery of the disease. Thus, it will be of good interest to perform deep sequencing of this region to look for the causal variant of stroke in the population. It may also be beneficial to study changes in the expression of NINJ2 in brains of post-mortem ischemic stroke patients carrying the SNPs associated with greater risk of stroke in order to correlate the findings in mice with humans. A change in the expression of NINJ2 in human brains will be a valid parallel comparison to the known changes observed in mice brains.

It is hypothesized that the knockout of Ninj2 may increase the susceptibility of brain damage due to ischemic stroke. An animal model that has being genetically

modified permits the analysis of the biological mechanisms underlying the cause for the disease (Bonthu S. et al., 1997). If shown to increase susceptibility to damage in the brain of the Ninj2-KO mice, Ninj2 could be classified as a major molecular target that contributes to neuroprotection (a.k.a. neurovascular remodeling). It is also suggested that NINJ2 gene is an endogenous target of recovery that is silenced by unknown mechanisms that could be associated with the stroke-associated SNPs in the population. Elucidating these mechanisms can be beneficial for the design of personal medicine for the prevention of stroke in patients with high probability of developing the disease. This study provides a better understanding for the involvement of NINJ2 in stroke.

APPENDIX

PREPARATION OF SOLUTIONS

Master-Mix preparation for cDNA production - A master mix including all the reagents from the following table was prepared in ice.

Table A.1 Preparation of the cDNA reaction from the ABI RT Kit

10X RT Buffer	2.0 µl
25X dNTP Mix (100uM)	0.8 µl
10X RT Random Primers	2.0 µl
Multiscribe R. Transcriptase	1.0 µl
Nuclease-free H2O	4.2 µl
Total	**9.0 µl**

It is considered more accurate to prepare a master mix for all the reactions prepared in that day. For instance, if all the 19 brain RNA samples are used that day to make cDNA, then a master mix of 19 + 10% of 19 +1 samples are prepared. This master mix is enough to prepare 21 cDNA samples.

qPCR Analysis– The 7900 ABI qPCR instrument yields a C_T value for each well in 96-well plate. The C_T values are transported to our spreadsheet template in Microsoft Excel linked to the templates in Figure A.2. Our qPCR analysis program in Excel performs further analysis on the C_T values. This design permits the user to input the desired amount, the identity of the gene, and the timeline of experimentation in an Excel worksheet. The program automatically connects this information into a printable design for qPCR plate. Our plate format follows the requirements for an RQ analysis. These plates are color coded so as to represent a sample ID with a different color. The 3 days sample is repeated in both plates in order to maintain consistency between the time-points. This worksheet uses the same format as the one provided by the ABI instrumentation, thus facilitating data analysis. Figure A.2 shows 96-well plates designed using advanced functions in Excel.

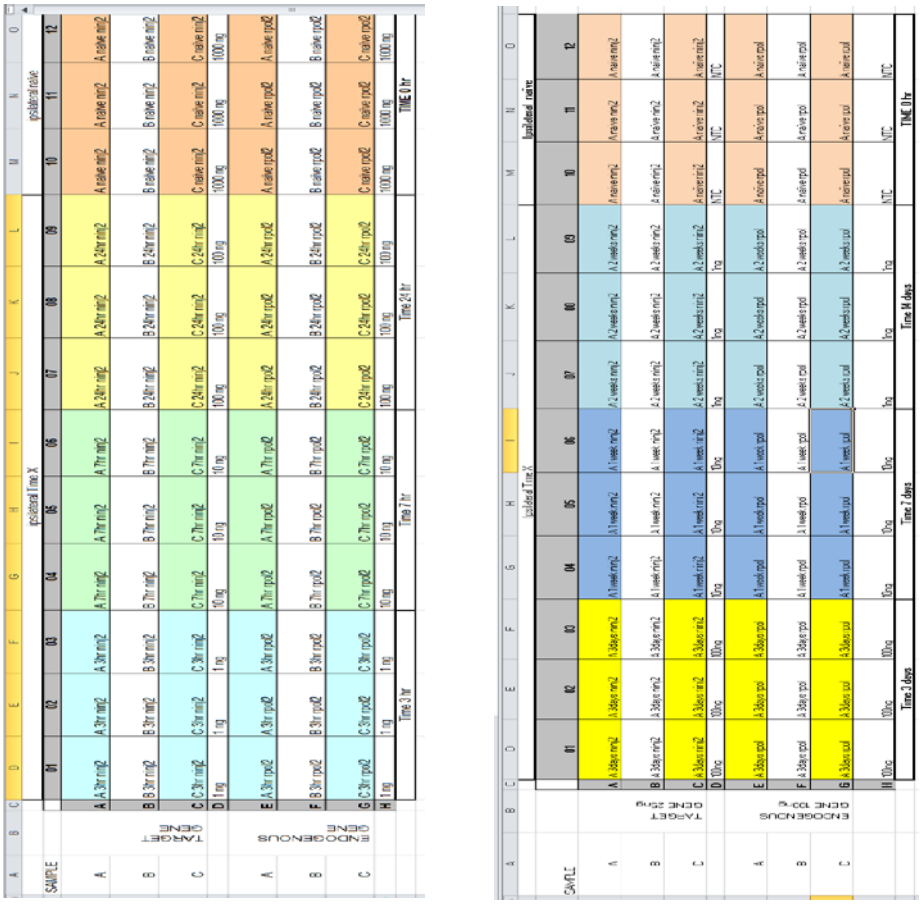

Figure A.1: Automated qPCR plates (Injury and Recovery) designed using Excel.

cDNA Input – The same cDNA aliquots are used for the rows corresponding to the target gene (rows A – D) and the endogenous gene (rows E – H) probes. For instance, wells A1-A3 receive both 1µl of cDNA and 8µl of water. cDNA molecules from the same aliquot are added into wells D1-D3. Then, 11 µl of the qPCR master mix containing 1 µl of the corresponding primer/probe are added onto each of these wells. In this way, both groups receive equal treatment and the degree of error between triplicates and gene probes is significantly reduced. The 96-well plate also includes negative control wells (NTC) wells with the water used in the preparation of the reactions. These wells signal when the reactions carry contaminants which may interfere with the results.

Standard Curve – Figure A.2 shows one example of a standard curve generated by the SDS software. Its slope is used to calculate the amplification efficiency of RPOL2.

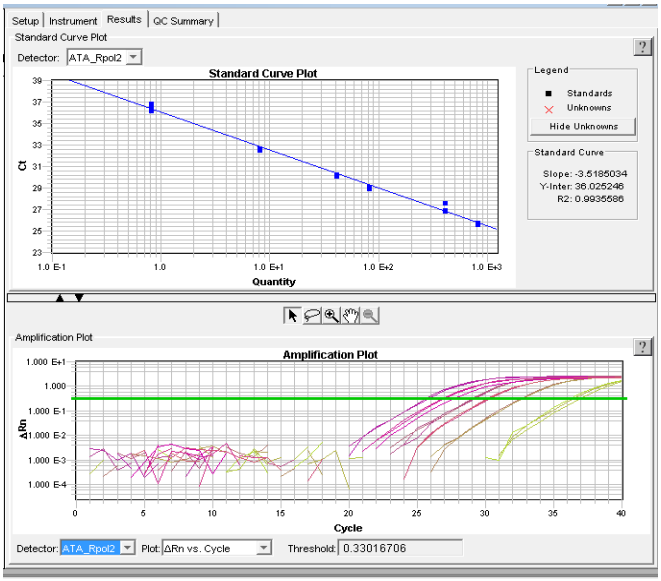

Figure A.2 Standard Curve Plot and Amplification Plot showing a serial dilution with cDNA from healthy mouse brain cortex. The amplification plot shows a green horizontal line that indicates where the C_T value lies at the exponential phase of the sigmoidal curves.

Details of qPCR Amplification Efficiencies per experiment – Table 3.1 shows the qPCR efficiency data for all the three experimental runs of the target (NINJ2 and INOS2) and endogenous gene (RPOL2). Most of our data meet the initial presumption of equal PCR efficiency as required by the • -Ct method.

Table 3.1 qPCR Amplification efficiencies per qPCR experiment.

A NINJ2 IPSILATERAL

		INJURY PLATE			
		qPCR Amplification Efficiencies			
		Sample	Slope	log E	E
EXP1	NINJ2	Naïve	-3.45	0.290	94.82
	RPOL2	Naïve	-3.62	0.277	89.03
EXP2	NINJ2	Naïve	-3.30	0.303	100.79
	RPOL2	Naïve	-3.35	0.299	98.91
EXP3	NINJ2	Naïve	-3.42	0.292	96.08
	RPOL2	Naïve	-3.52	0.284	92.45
		RECOVERY PLATE			
		qPCR Amplification Efficiencies			
		Sample	Slope	log E	E
EXP1	NINJ2	Naïve	-2.01	0.498	214.79
	RPOL2	Naïve	-3.48	0.287	93.79
EXP2	NINJ2	Naïve	-3.33	0.300	99.51
	RPOL2	Naïve	-2.92	0.343	120.20
EXP3	NINJ2	Naïve	-3.34	0.300	99.38
	RPOL2	Naïve	-3.48	0.287	93.67

B NINJ2 CONTRALATERAL

		INJURY PLATE			
		PCR Efficiency			
			Slope	log E	E
EXP1	NINJ2	Naïve	-3.26	0.306	102.48
	RPOL2	Naïve	-3.45	0.290	95.05
EXP2	NINJ2	Naïve	-3.26	0.306	102.48
	RPOL2	Naïve	-3.45	0.290	95.05
EXP3	NINJ2	Naïve	-3.40	0.294	97.00
	RPOL2	Naïve	-3.36	0.297	98.27
		RECOVERY PLATE			
		PCR Efficiency			
			Slope	log E	E
EXP1	NINJ2	Naïve	-3.55	0.282	91.37
	RPOL2	Naïve	-3.42	0.292	95.91
EXP2	NINJ2	Naïve	-3.30	0.303	100.96
	RPOL2	Naïve	-3.50	0.286	93.12
EXP3	NINJ2	Naïve	-3.13	0.320	108.86
	RPOL2	Naïve	-3.26	0.307	102.72

C INOS2 IPSILATERAL

		INJURY PLATE			
		PCR Efficiency			
			Slope	log E	E
EXP1	INOS2	Naïve	-2.290	0.437	173.33
	RPOL2	Naïve	-3.220	0.311	104.44
EXP2	INOS2	Naïve	-2.060	0.485	205.80
	RPOL2	Naïve	-3.520	0.284	92.35
EXP3	INOS2	Naïve	-2.220	0.450	182.13
	RPOL2	Naïve	-3.520	0.284	92.35
		RECOVERY PLATE			
		PCR Efficiency			
			Slope	log E	E
EXP1	INOS2	Naïve	-3.26	0.307	102.59
	RPOL2	Naïve	-3.45	0.290	94.82
EXP2	INOS2	Naïve	-3.70	0.270	86.19
	RPOL2	Naïve	-3.29	0.304	101.18
EXP3	INOS2	Naïve	-3.49	0.287	93.43
	RPOL2	Naïve	-3.41	0.293	96.47

D INOS2 CONTRALATERAL

		INJURY PLATE			
		PCR Efficiency			
			Slope	log E	E
EXP1	INOS2	Naïve	-3.196	0.313	105.53
	RPOL2	Naïve	-3.392	0.295	97.14
EXP2	INOS2	Naïve	0.044	-22.506	-100.00
	RPOL2	Naïve	-3.520	0.284	92.35
EXP3	INOS2	Naïve	-3.260	0.307	102.65
	RPOL2	Naïve	-3.520	0.284	92.35
		RECOVERY PLATE			
		PCR Efficiency			
			Slope	log E	E
EXP1	INOS2	Naïve	0.000	#DIV/0!	#DIV/0!
	RPOL2	Naïve	#NUM!	#NUM!	#NUM!
EXP2	INOS2	Naïve	-2.53	0.395	148.37
	RPOL2	Naïve	-3.42	0.292	95.97
EXP3	INOS2	Naïve	-3.20	0.312	105.24
	RPOL2	Naïve	-3.42	0.292	95.96

qPCR amplification efficiencies of INOS2 – The results for the qPCR amplification efficiencies of INOS2 are presented below. These show an efficiency of +/- 100%, suggesting that the $2^{-\bullet\bullet}{}_{T}$ method can be implemented for the calculation of the RQ of INOS2 following the timeline after a stroke.

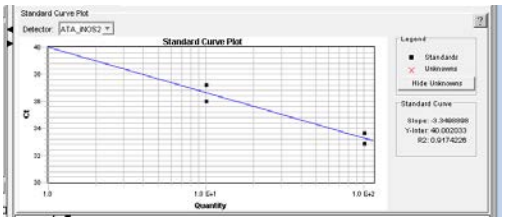

Figure A.3 Independent INOS2 Standard Curve Slope = -3.35 E =

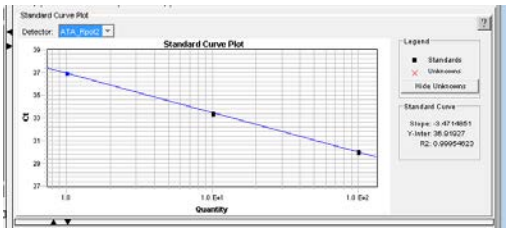

Figure A.4 Independent RPOL2 Standard Curve Slope = -3.47 E =

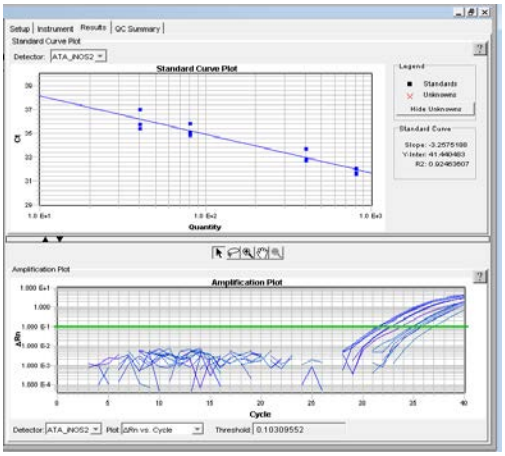

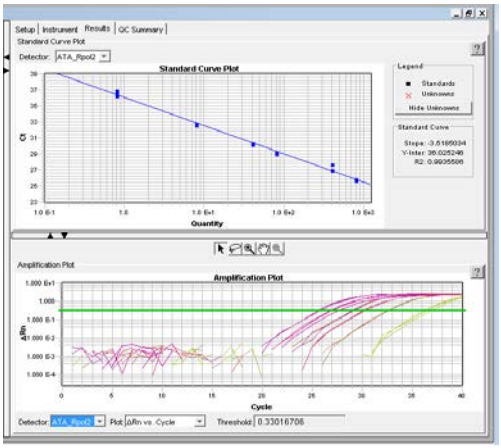

PCR Efficiency			
	Slope	log E	E
Naïve	-3.26	0.306748466	102.650867

PCR Efficiency			
	Slope	log E	E
Naïve	-3.52	0.284090909	92.349432

Figure A.5 Independent experiments for INOS2 and RPOL2 Standard Curves

Figure A.6 SAS Results from the mixed model test of statistics. These results demonstrate the adjusted p-values for the differences in the means of RQ values between time-points. These values control for the

replicates within the time-points. The values marked in yellow represent those that show significant differences in gene expression.

PROTEIN ANALYSIS

Mice tagging – Mice are tagged in their ear lobes and a record is maintained with the time at which the last CBF is measured. The time count starts at this stage for the subsequent brain dissection.

1X PBS – 1X PBS is diluted from 10X PBS with deionized water. The 10X PBS is prepared in 1 liter using the following reagents: 80g of NaCl, 2g of KCl, 14.4 g of Na2HPO4, and 2.4 g of KH2PO4. The dry chemicals are first dissolved in 800 ml of dH2O, pH adjusted to 7.4 with HCl, raised the volume to 1 liter, and autoclaved.

12% Electrophoretic Gel – First, 500 ml of 1.5M Tris-Borate (TB) and 500 ml of 0.5M TB is prepared with distilled water and saved in large glass containers. The 1.5M Tris Buffer (pH 8.8) is prepared for the resolving gel, while the 0.5 M Tris Buffer (pH 6.8) is prepared for the stacking gel. The 1.5M Tris Buffer is prepared by adding 90.85 g Tris into a total volume of 500 ml with dH2O, adjusting the pH to 8.8 with 1M HCl. The 0.5 M Tris Buffer is prepared by adding 30.28 g of Tris into a total volume of 500 ml with dH2O, adjusting the pH to 6.8 with 1M HCl. Both solutions are stored at 4oC. An Erlenmeyer flask is used to mix 4.0 ml of 30% acrylamide/Bisacrylamide, 2.5 ml of 1.5 M TB (pH 8.8), 3.35 ml H2O, 100µl of 10% SDS, 50µl of 10% AP, 10µl of TEMED for the Resolving Gel. The 10% AP is prepared with 0.5 g AP and dH2O to 5 ml and stored at 4oC for no more than 2 weeks.

4% Stacking Gel – The 4% Stacking gel is prepared with 0.65 ml of 30% acrylamide/Bis, 1.25 ml of 0.5M TB (pH6.8), 3.05 ml of H2O, 50 µl of 10% SDS, 25 µl of 10% Ammonium Persulfate (AP), and 5ul of TEMED. The resolving gel is casted first, then a layer of water is added on top to demarcate the end of the polymerization, and then the stacking gel is casted on top. The comb is then placed on the stacking gel to mark the wells for the samples.

4X Loading Stock Solution – To make the 4X stock, 2ml of 0.5M TB (pH 6.8), 0.31g of DTT, 0.4g of SDS, and 0.002 g of 0.2% Bromophenol Blue, and 2 ml of Glycerol are mixed in a 15 ml conical tube. To make 1X from 4X stock, the loading buffer is diluted 1:3 times with the sample in RIPA buffer. The final 1X concentration for the loading buffer reagents are 50mM Tris-HCl, 0.1M DTT, 2.0% SDS, 0.01% Bb, and 10% Glycerol.

Preparation of Lysis (RIPA) Buffer – (50mM Tris-HCl, 1% NP-40, 0.5% deoxycholic acid, 0.1% SDS, 1mM EDTA, and 150 mM NaCl).

Making the TBST – The final solution of TBST contains 10mM Tris-HCl, 100 mM NaCl, and 0.2% Tween 20. These solutions are prepared directly from the stock chemicals as followed: 1.2 g of Tris-HCl mixed with 5.8g of NaCl and 2ml of Tween 20 all added into ddH2O to 1000 ml and pH adjusted to 7.4.

Protein Gel Electrophoresis –The first step in the procedure involves running the gel in Tris-glycine electrophoresis buffer (pH 8.3) at 70V for about 15 minutes, then at 130V for 2 hours or until the purple/bluish mark from the bromophenol blue reaches the bottom. The Tris-glycine buffer is prepared with 0.025 M Tris, 0.1 M glycine, and 0.1%

SDS. Running the gel at a lower voltage prevents the high electric shock to disrupt some of the most sensitive proteins. As the SDS-coated (negatively charged) proteins migrate towards the positive end of the gel, they are compartmentalized in holes formed by a mesh of bis-acrylamide polymers in the gel. The holes are proportional to the size of proteins. Proteins of bigger size will remain stuck on top of the gel. The Precision plus Protein Standard (dual color) from BioRad is also used to determine the molecular size of our protein of interest. Proteins in the gel are then transferred onto a pvdf membrane for further testing with the antibody.

Protein transfer (part 1)– The transfer of proteins into a membrane involves making a "sandwich" system with the gel containing the protein samples; as well as the corresponding pvdf membranes and filter pads, made out of nylon sponge, placed on either side of the gel. This system runs in an electro-active solution (Tris-buffered saline + Tween20 or TBS-T) in ice and in the cold room in order to transfer the proteins onto a membrane with minimal disruption to the protein structures.

Protein transfer (part 2)– Preparing for the protein transfer procedure requires wetting the PVDF membrane in 100% methanol for 30 sec and then placing it inside a chamber with the transfer buffer. The filter pad, as well as the transfer apparatus and the gloves, are also soaked in transfer buffer. The "sandwich" is set up so that the positively charge side is underneath the membrane holding the protein gel on top. The use of filters prevents leakage of proteins outside of the membrane. The filter pad is placed first, followed by the PVDF membrane, the protein gel, and another filter pad on top. For every layer of material added onto the system, a cylindrical tube is used to flatten out the transfer units so as to avoid the formation of air bubbles. Once the system is

constructed, a 25 V current is produced overnight for the proteins to transfer onto the pvdf membrane at 4oC. The transfer apparatus is disassembled, and the pvdf membrane is taken to wash in a dish with multiple washes of H2O.

Protein Visualization – Ponceau S stain from Sigma is used to stain the membrane and visualize the transfer of proteins in the following way. The membrane is immersed in sufficient Ponceau S Staining Solution and stained for 5 minutes. The membrane is then rinsed with distilled water until the background is clear.

Clearing of the Ponceau Stain – After proteins are visualized, the membrane is rinsed in an aqueous solution of 0.1M NaOH. The membrane is then rinsed with running distilled water for 2-3 minutes, and is ready to be used for immunological detection. A pencil is used to mark over the bands from the marker lane to ensure the proper location of the molecular sizes. The excess of membrane is trimmed away and rinsed for 5 minutes in PBSt buffer.

Antibody Incubation – The membrane blot is incubated in 1:500 of the P. Tech primary Antibody overnight in the cold room on a shaker. The final volume (greater than or equal to 2 ml) is prepared so that it would sufficiently immerse the membrane in solution and prevent drying out the membrane. The chamber of incubation is covered with an aluminum foil to prevent evaporation. The following day, the blot is rinsed with 3 changes of TBS-tr (2X 5 min, 1X 15 min) on a shaker. The membrane is then incubated with anti-rabbit 2nd Ab conjugated with HRP with the optimized dilution of 1:2000 in blocking buffer. This is incubated for 1 hour at room temperature on a shaker

with sufficient volume to cover the membrane and prevent it from drying out. The blot is then rinsed with 3 change of PBSt (2X2 min, 1X15 min) on a shaker at high speed.

Film Developing – The film developing procedure is done inside a dark room following regular lab protocol with a filtered film box in the dark. Basically, the Super-Signal West Dura Extended Duration Substrate from Thermo Fisher is first prepared with 1:1 ratio of the solution A and solution B in the kit just prior to its use. The transfer membrane is transferred onto a plastic sheet and the prepared ECL mixture is added onto it and allowed to react for 5 minutes, making sure not to let any part of the membrane dry out. The membrane is then covered with the same plastic sheet and taped inside of the developing cassette. An absorbent tissue is used to remove excess liquid and press out any bubbles from between the blot and the membrane filter.

Membrane Stripping – The membrane is stripped with a mild stripping buffer (pH 2.2) consisting of 15 g glycine, 1g SDS, 10ml Tween 20. The process followed for stripping the membrane is by discarding the solution in between each of the following steps: 10 minutes incubation, 10 minutes PBS, 10 minutes PBS, 10 minutes PBS, 5 minutes TBST (0.1%), and 5 minutes on TBST (0.1%) again.

Protein quantification results – Changes in the protein levels of NINJ2 are quantified using the ratio of the relative densities of the signals in the western blots. The raw data from ImageJ along with details of the normalized relative density (NRD) calculation and t-test results are shown below.

References

(1993). "Secondary prevention in non-rheumatic atrial fibrillation after transient ischaemic attack or minor stroke. EAFT (European Atrial Fibrillation Trial) Study Group." Lancet 342(8882): 1255-62.

(1995). "Endarterectomy for asymptomatic carotid artery stenosis. Executive Committee for the Asymptomatic Carotid Atherosclerosis Study." Jama 273(18): 1421-8.

(2007). "Prevalence of stroke--United States, 2005." MMWR Morb Mortal Wkly Rep 56(19): 469-74.

Aboa-Eboulé C, Béjot Y, Osseby GV, Rouaud O, Binquet C, Marie C, Cottin Y, Giroud M, Bonithon-Kopp C. (2011). "Influence of prior transient ischaemic attack on stroke prognosis." J Neurol Neurosurg Psychiatry 82(9): 993-1000.

Adams HP Jr, Bendixen BH, Kappelle LJ, Biller J, Love BB, Gordon DL, Marsh EE 3rd. (1993). "Classification of subtype of acute ischemic stroke. Definitions for use in a multicenter clinical trial. TOAST. Trial of Org 10172 in Acute Stroke Treatment." Stroke 24(1): 35-41.

Altschul SF, Madden TL, Schäffer AA, Zhang J, Zhang Z, Miller W, Lipman DJ. (1997). "Gapped BLAST and PSI-BLAST: a new generation of protein database search programs." Nucleic Acids Res 25(17): 3389-402.

Amarenco P, Duyckaerts C, Tzourio C, Hénin D, Bousser MG, Hauw JJ. (1992). "The prevalence of ulcerated plaques in the aortic arch in patients with stroke." N Engl J Med 326(4): 221-5.

Arai AC, Xia YF, Suzuki E. (2004). "Modulation of AMPA receptor kinetics differentially influences synaptic plasticity in the hippocampus." Neuroscience 123(4): 1011-24.

Araki, T. and J. Milbrandt (1996). "Ninjurin, a novel adhesion molecule, is induced by nerve injury and promotes axonal growth." Neuron 17(2): 353-61.

Araki, T. and J. Milbrandt (2000). "Ninjurin2, a novel homophilic adhesion molecule, is expressed in mature sensory and enteric neurons and promotes neurite outgrowth." J Neurosci 20(1): 187-95.

Araki T, Zimonjic DB, Popescu NC, Milbrandt J. (1997). "Mechanism of homophilic binding mediated by ninjurin, a novel widely expressed adhesion molecule." J Biol Chem 272(34): 21373-80.

Aroniadou-Anderjaska V, Fritsch B, Qashu F, Braga MF. (2008). "Pathology and pathophysiology of the amygdala in epileptogenesis and epilepsy." Epilepsy Res 78(2-3): 102-16.

Arrick DM, Sharpe GM, Sun H, Mayhan WG. (2007). "nNOS-dependent reactivity of cerebral arterioles in Type 1 diabetes." Brain Res 1184: 365-71.

Astrup J, Symon L, Branston NM, Lassen NA. (1977). "Cortical evoked potential and extracellular K+ and H+ at critical levels of brain ischemia." Stroke 8(1): 51-7.

Bacigaluppi M, Comi G, Hermann DM. "Animal models of ischemic stroke. Part one: modeling risk factors." Open Neurol J 4: 26-33.

Bak S, Gaist D, Sindrup SH, Skytthe A, Christensen K. (2002). "Genetic liability in stroke: a long-term follow-up study of Danish twins." Stroke 33(3): 769-74.

Bamford J, Sandercock P, Dennis M, Burn J, Warlow C. (1991). "Classification and natural history of clinically identifiable subtypes of cerebral infarction." Lancet 337(8756): 1521-6.

Bazan NG, Marcheselli VL, Cole-Edwards K. (2005). "Brain response to injury and neurodegeneration: endogenous neuroprotective signaling." Ann N Y Acad Sci 1053: 137-47.

Benfey, M. and A. J. Aguayo (1982). "Extensive elongation of axons from rat brain into peripheral nerve grafts." Nature 296(5853): 150-2.

Berrouschot J, Sterker M, Bettin S, Köster J, Schneider D. (1998). "Mortality of space-occupying ('malignant') middle cerebral artery infarction under conservative intensive care." Intensive Care Med 24(6): 620-3.

Bonita, R. (1992). "Epidemiology of stroke." Lancet 339(8789): 342-4.

Bonita R, Solomon N, Broad JB. (1997). "Prevalence of stroke and stroke-related disability. Estimates from the Auckland stroke studies." Stroke 28(10): 1898-902.

Bonthu S, Heistad DD, Chappell DA, Lamping KG, Faraci FM. "Atherosclerosis, vascular remodeling, and impairment of endothelium-dependent relaxation in genetically altered hyperlipidemic mice." Arterioscler Thromb Vasc Biol 17(11): 2333-40.

Borsello T, Clarke PG, Hirt L, Vercelli A, Repici M, Schorderet DF, Bogousslavsky J, Bonny C. (2003). "A peptide inhibitor of c-Jun N-terminal kinase protects against excitotoxicity and cerebral ischemia." Nat Med 9(9): 1180-6.

Brass LM, Isaacsohn JL, Merikangas KR, Robinette CD. (1992). "A study of twins and stroke." Stroke 23(2): 221-3.

Brott, T. and J. Bogousslavsky (2000). "Treatment of acute ischemic stroke." N Engl J Med 343(10): 710-22.

Brouns R, Sheorajpanday R, Wauters A, De Surgeloose D, Mariën P, De Deyn PP. (2008). "Evaluation of lactate as a marker of metabolic stress and cause of secondary damage in acute ischemic stroke or TIA." Clin Chim Acta 397(1-2): 27-31.

Caplan, L.R. (1998). “Prevention of strokes and recurrent strokes.” J Neurol Neurosurg Psychiatry 64: 716.

Cedarbaum, J. M. and J. P. Blass (1986). "Mitochondrial dysfunction and spinocerebellar degenerations." Neurochem Pathol 4(1): 43-63.

Chen C, Ridzon DA, Broomer AJ, Zhou Z, Lee DH, Nguyen JT, Barbisin M, Xu NL, Mahuvakar VR, Andersen MR, Lao KQ, Livak KJ, Guegler KJ. (2005). "Real-time quantification of microRNAs by stem-loop RT-PCR." Nucleic Acids Res 33(20): e179.

Chen R, Qiu W, Liu Z, Cao X, Zhu T, Li A, Wei Q, Zhou J. (2007). "Identification of JWA as a novel functional gene responsive to environmental oxidative stress induced by benzo[a]pyrene and hydrogen peroxide." Free Radic Biol Med 42(11): 1704-14.

Cheng YD, Al-Khoury L, Zivin JA.. (2004). "Neuroprotection for ischemic stroke: two decades of success and failure." NeuroRx 1(1): 36-45.

Chiba T, Itoh T, Tabuchi M, Satou T, Ezaki O.. (2009). "Dietary protein, but not carbohydrate, is a primary determinant of the onset of stroke in stroke-prone spontaneously hypertensive rats." Stroke 40(8): 2828-35.

Chong ZZ, Xu QP, Sun JN. (2001). "Effects and mechanisms of triacetylshikimic acid on platelet adhesion to neutrophils induced by thrombin and reperfusion after focal cerebral ischemia in rats." Acta Pharmacol Sin 22(8): 679-84.

Chukwudelunzu FE, Meschia JF, Graff-Radford NR, Lucas JA. (2001). "Extensive metabolic and neuropsychological abnormalities associated with discrete infarction of the genu of the internal capsule." J Neurol Neurosurg Psychiatry 71(5): 658-62.

Collins FS, Guyer MS, Charkravarti A. (1997). "Variations on a theme: cataloging human DNA sequence variation." Science 278(5343): 1580-1.

Dirnagl U, Simon RP, Hallenbeck JM. (2003). "Ischemic tolerance and endogenous neuroprotection." Trends Neurosci 26(5): 248-54.

Dugan, L. L. and D. W. Choi (1994). "Excitotoxicity, free radicals, and cell membrane changes." Ann Neurol 35 Suppl: S17-21.

Durukan, A. and T. Tatlisumak (2007). "Acute ischemic stroke: overview of major experimental rodent models, pathophysiology, and therapy of focal cerebral ischemia." Pharmacol Biochem Behav 87(1): 179-97.

Fisher, C. M. (1979). "Capsular infarcts: the underlying vascular lesions." Arch Neurol 36(2): 65-73.

Fisher, C. M. and R. G. Ojemann (1986). "A clinico-pathologic study of carotid endarterectomy plaques." Rev Neurol (Paris) 142(6-7): 573-89.

Fu, S. Y. and T. Gordon (1997). "The cellular and molecular basis of peripheral nerve regeneration." Mol Neurobiol 14(1-2): 67-116.

García-Bonilla L, Rosell A, Torregrosa G, Salom JB, Alborch E, Gutiérrez M, Díez-Tejedor E, Martínez-Murillo R, Agulla J, Ramos-Cabrer P, Castillo J, Gasull T, Montaner J. "Recommendations guide for experimental animal models in stroke research." Neurologia 26(2): 105-110.

Gaudet AD, Popovich PG, Ramer MS. "Wallerian degeneration: gaining perspective on inflammatory events after peripheral nerve injury." J Neuroinflammation 8: 110.

Good, D. C. (1990). "Cerebrovascular Disease."

Greenberg, D. A. (1993). "Linkage analysis of "necessary" disease loci versus "susceptibility" loci." Am J Hum Genet 52(1): 135-43.

Griffin, J. W. and W. J. Thompson (2008). "Biology and pathology of nonmyelinating Schwann cells." Glia 56(14): 1518-31.

Gross, S. B. (1995). "Transient ischemic attacks (TIA): current issues in diagnosis and management." J Am Acad Nurse Pract 7(7): 329-37.

Guo, S. W. (1998). "Inflation of sibling recurrence-risk ratio, due to ascertainment bias and/or overreporting." Am J Hum Genet 63(1): 252-8.

Hacke W, Schwab S, Horn M, Spranger M, De Georgia M, von Kummer R. (1996). "'Malignant' middle cerebral artery territory infarction: clinical course and prognostic signs." Arch Neurol 53(4): 309-15.

Hademenos, G. J. and T. F. Massoud (1997). "Biophysical mechanisms of stroke." Stroke 28(10): 2067-77.

Hanis CL, Boerwinkle E, Chakraborty R, Ellsworth DL, Concannon P, Stirling B, Morrison VA, Wapelhorst B, Spielman RS, Gogolin-Ewens KJ, Shepard JM, Williams SR, Risch N, Hinds D, Iwasaki N, Ogata M, Omori Y, Petzold C, Rietzch H, Schröder HE, Schulze J, Cox NJ, Menzel S, Boriraj VV, Chen X, Lim LR, Lindner T, Mereu LE, Wang YQ, Xiang K, Yamagata K, Yang Y, Bell GI. (1996). "A genome-wide search for human non-insulin-dependent (type 2) diabetes genes reveals a major susceptibility locus on chromosome 2." Nat Genet 13(2): 161-6.

Hankey, G. J. and C. P. Warlow (1999). "Treatment and secondary prevention of stroke: evidence, costs, and effects on individuals and populations." Lancet 354(9188): 1457-63.

Hart RG, Benavente O, McBride R, Pearce LA. (1999). "Antithrombotic therapy to prevent stroke in patients with atrial fibrillation: a meta-analysis." Ann Intern Med 131(7): 492-501.

Heintz, N. (1993). "Cell death and the cell cycle: a relationship between transformation and neurodegeneration?" Trends Biochem Sci 18(5): 157-9.

Hellemans J, Mortier G, De Paepe A, Speleman F, Vandesompele J. (2007). "qBase relative quantification framework and software for management and automated analysis of real-time quantitative PCR data." Genome Biol 8(2): R19.

Hirsch, E. C. (1993). "Does oxidative stress participate in nerve cell death in Parkinson's disease?" Eur Neurol 33 Suppl 1: 52-9.

Hu G, Sarti C, Jousilahti P, Silventoinen K, Barengo NC, Tuomilehto J. (2005). "Leisure time, occupational, and commuting physical activity and the risk of stroke." Stroke 36(9): 1994-9.

Hu G, Tuomilehto J, Silventoinen K, Sarti C, Männistö S, Jousilahti P. (2007). "Body mass index, waist circumference, and waist-hip ratio on the risk of total and type-specific stroke." Arch Intern Med 167(13): 1420-7.

Huntley GW, Vickers JC, Morrison JH. (1994). "Cellular and synaptic localization of NMDA and non-NMDA receptor subunits in neocortex: organizational features related to cortical circuitry, function and disease." Trends Neurosci 17(12): 536-43.

Huttner, H. B. and S. Schwab (2009). "Malignant middle cerebral artery infarction: clinical characteristics, treatment strategies, and future perspectives." Lancet Neurol 8(10): 949-58.

Ikram, M. A., S. Seshadri, et al. (2009). "Genomewide association studies of stroke." N Engl J Med 360(17): 1718-28.

Jessen, K. R. and R. Mirsky "Control of Schwann cell myelination." F1000 Biol Rep 2.

Jin K, Wang X, Xie L, Mao XO, Zhu W, Wang Y, Shen J, Mao Y, Banwait S, Greenberg DA. (2006). "Evidence for stroke-induced neurogenesis in the human brain." Proc Natl Acad Sci U S A 103(35): 13198-202.

Johnson, A. D. and C. J. O'Donnell (2009). "An open access database of genome-wide association results." BMC Med Genet 10: 6.

Jones TH, Morawetz RB, Crowell RM, Marcoux FW, FitzGibbon SJ, DeGirolami U, Ojemann RG. (1981). "Thresholds of focal cerebral ischemia in awake monkeys." J Neurosurg 54(6): 773-82.

Joung I, Yoo M, Woo JH, Chang CY, Heo H, Kwon YK. "Secretion of EGF-like domain of heregulinbeta promotes axonal growth and functional recovery of injured sciatic nerve." Mol Cells 30(5): 477-84.

Joutel A, Corpechot C, Ducros A, Vahedi K, Chabriat H, Mouton P, Alamowitch S, Domenga V, Cécillion M, Maréchal E, Maciazek J, Vayssière C, Cruaud C, Cabanis EA, Ruchoux MM, Weissenbach J, Bach JF, Bousser MG, Tournier-Lasserve E. (1997). "Notch3 mutations in cerebral autosomal dominant arteriopathy with subcortical infarcts and leukoencephalopathy (CADASIL), a mendelian condition causing stroke and vascular dementia." Ann N Y Acad Sci 826: 213-7.

Kannel WB, Wolf PA, Verter J, McNamara PM.. (1970). "Epidemiologic assessment of the role of blood pressure in stroke. The Framingham study." Jama 214(2): 301-10.

Kaplan B, Brint S, Tanabe J, Jacewicz M, Wang XJ, Pulsinelli W. (1991). "Temporal thresholds for neocortical infarction in rats subjected to reversible focal cerebral ischemia." Stroke 22(8): 1032-9.

Katsura K, Kristián T, Nair R, Siesjö BK. (1994). "Regulation of intra- and extracellular pH in the rat brain in acute hypercapnia: a re-appraisal." Brain Res 651(1-2): 47-56.

Katsura K, Kristián T, Siesjö BK. (1994). "Energy metabolism, ion homeostasis, and cell damage in the brain." Biochem Soc Trans 22(4): 991-6.

Kendler KS, Neale MC, Kessler RC, Heath AC, Eaves LJ. (1993). "A test of the equal-environment assumption in twin studies of psychiatric illness." Behav Genet 23(1): 21-7.

Khaw, K. T. (1996). "Epidemiology of stroke." J Neurol Neurosurg Psychiatry 61(4): 333-8.

Kidwell CS, Saver JL, Mattiello J, Starkman S, Vinuela F, Duckwiler G, Gobin YP, Jahan R, Vespa P, Kalafut M, Alger JR (2000). "Thrombolytic reversal of acute human cerebral ischemic injury shown by diffusion/perfusion magnetic resonance imaging." Ann Neurol 47(4): 462-9.

Kiely DK, Wolf PA, Cupples LA, Beiser AS, Myers RH. (1993). "Familial aggregation of stroke. The Framingham Study." Stroke 24(9): 1366-71.

Kolko M, Bruhn T, Christensen T, Lazdunski M, Lambeau G, Bazan NG, Diemer NH.. (1999). "Secretory phospholipase A2 potentiates glutamate-induced rat striatal neuronal cell death in vivo." Neurosci Lett 274(3): 167-70.

Lammie GA, Brannan F, Slattery J, Warlow C. (1997). "Nonhypertensive cerebral small-vessel disease. An autopsy study." Stroke 28(11): 2222-9.

Lawes CM, Bennett DA, Feigin VL, Rodgers A.. (2004). "Blood pressure and stroke: an overview of published reviews." Stroke 35(4): 1024.

Lawes CM, Parag V, Bennett DA, Suh I, Lam TH, Whitlock G, Barzi F, Woodward M; Asia Pacific Cohort Studies Collaboration. (2004). "Blood glucose and risk of cardiovascular disease in the Asia Pacific region." Diabetes Care 27(12): 2836-42.

Lee HJ, Ahn BJ, Shin MW, Choi JH, Kim KW.. "Ninjurin1: a potential adhesion molecule and its role in inflammation and tissue remodeling." Mol Cells 29(3): 223-7.

Lewandowski CA, Rao CP, Silver B. (2008). "Transient ischemic attack: definitions and clinical presentations." Ann Emerg Med 52(2): S7-16.

Liao D, Cooper L, Cai J, Toole JF, Bryan NR, Hutchinson RG, Tyroler HA. (1996). "Presence and severity of cerebral white matter lesions and hypertension, its treatment, and its control. The ARIC Study. Atherosclerosis Risk in Communities Study." Stroke 27(12): 2262-70.

Liao D, Myers R, Hunt S, Shahar E, Paton C, Burke G, Province M, Heiss G. (1997). "Familial history of stroke and stroke risk. The Family Heart Study." Stroke 28(10): 1908-12.

Liu, W. and D. A. Saint (2002). "A new quantitative method of real time reverse transcription polymerase chain reaction assay based on simulation of polymerase chain reaction kinetics." Anal Biochem 302(1): 52-9.

Livak, K. J. and T. D. Schmittgen (2001). "Analysis of relative gene expression data using real-time quantitative PCR and the 2(-Delta Delta C(T)) Method." Methods 25(4): 402-8.

Lloyd-Jones D, Adams R, Carnethon M, De Simone G, Ferguson TB, Flegal K, Ford E, Furie K, Go A, Greenlund K, Haase N, Hailpern S, Ho M, Howard V, Kissela B, Kittner S, Lackland D, Lisabeth L, Marelli A, McDermott M, Meigs J, Mozaffarian D, Nichol G, O'Donnell C, Roger V, Rosamond W, Sacco R, Sorlie P, Stafford R, Steinberger J, Thom T, Wasserthiel-Smoller S, Wong N, Wylie-Rosett J, Hong Y; American Heart Association Statistics Committee and Stroke Statistics Subcommittee. (2009). "Heart disease and stroke statistics--2009 update: a report from the American Heart Association Statistics Committee and Stroke Statistics Subcommittee." Circulation 119(3): 480-6.

WRITING GROUP MEMBERS, Lloyd-Jones D, Adams RJ, Brown TM, Carnethon M, Dai S, De Simone G, Ferguson TB, Ford E, Furie K, Gillespie C, Go A, Greenlund K, Haase N, Hailpern S, Ho PM, Howard V, Kissela B, Kittner S, Lackland D, Lisabeth L, Marelli A, McDermott MM, Meigs J, Mozaffarian D, Mussolino M, Nichol G, Roger VL, Rosamond W, Sacco R, Sorlie P, Roger VL, Thom T, Wasserthiel-Smoller S, Wong ND, Wylie-Rosett J; American Heart Association Statistics Committee and Stroke Statistics Subcommittee. "Heart disease and stroke statistics--2010 update: a report from the American Heart Association." Circulation 121(7): e46-e215.

Lo, E. H. (2008). "Experimental models, neurovascular mechanisms and translational issues in stroke research." Br J Pharmacol 153 Suppl 1: S396-405.

Lo EH, Dalkara T, Moskowitz MA. (2003). "Mechanisms, challenges and opportunities in stroke." Nat Rev Neurosci 4(5): 399-415.

MacGregor AJ, Snieder H, Schork NJ, Spector TD. (2000). "Twins. Novel uses to study complex traits and genetic diseases." Trends Genet 16(3): 131-4.

MacMahon S, Peto R, Cutler J, Collins R, Sorlie P, Neaton J, Abbott R, Godwin J, Dyer A, Stamler J. (1990). "Blood pressure, stroke, and coronary heart disease. Part 1, Prolonged differences in blood pressure: prospective observational studies corrected for the regression dilution bias." Lancet 335(8692): 765-74.

Majid A, He YY, Gidday JM, Kaplan SS, Gonzales ER, Park TS, Fenstermacher JD, Wei L, Choi DW, Hsu CY. (2000). "Differences in vulnerability to permanent focal cerebral ischemia among 3 common mouse strains." Stroke 31(11): 2707-14.

Mancia G, Groppelli A, Casadei R, Omboni S, Mutti E, Parati G. (1990). "Cardiovascular effects of smoking." Clin Exp Hypertens A 12(5): 917-29.

Manolio, T. A. "Genomewide association studies and assessment of the risk of disease." N Engl J Med 363(2): 166-76.

Martin RL, Lloyd HG, Cowan AI. (1994). "The early events of oxygen and glucose deprivation: setting the scene for neuronal death?" Trends Neurosci 17(6): 251-7.

Minger SL, Ekonomou A, Carta EM, Chinoy A, Perry RH, Ballard CG. (2007). "A genome-wide genotyping study in patients with ischaemic stroke: initial analysis and data release." Lancet Neurol 6(5): 414-20.

McGue, M. (1992). "When assessing twin concordance, use the probandwise not the pairwise rate." Schizophr Bull 18(2): 171-6.

McMahon, H. T. and D. G. Nicholls (1990). "Glutamine and aspartate loading of synaptosomes: a reevaluation of effects on calcium-dependent excitatory amino acid release." J Neurochem 54(2): 373-80.

Minger SL, Ekonomou A, Carta EM, Chinoy A, Perry RH, Ballard CG. (2007). "Endogenous neurogenesis in the human brain following cerebral infarction." Regen Med 2(1): 69-74.

Mohammadi MT, Shid-Moosavi SM, Dehghani GA. "Contribution of nitric oxide synthase (NOS) in blood-brain barrier disruption during acute focal cerebral ischemia in normal rat." Pathophysiology.

Montgomery, S. B. and E. T. Dermitzakis (2009). "The resolution of the genetics of gene expression." Hum Mol Genet 18(R2): R211-5.

Murinson BB, Archer DR, Li Y, Griffin JW. (2005). "Degeneration of myelinated efferent fibers prompts mitosis in Remak Schwann cells of uninjured C-fiber afferents." J Neurosci 25(5): 1179-87.

Navaratna D, Guo S, Arai K, Lo EH. (2009). "Mechanisms and targets for angiogenic therapy after stroke." Cell Adh Migr 3(2): 216-23.

Nicholls, D. and D. Attwell (1990). "The release and uptake of excitatory amino acids." Trends Pharmacol Sci 11(11): 462-8.

Nicoli F, Lefur Y, Denis B, Ranjeva JP, Confort-Gouny S, Cozzone PJ. (2003). "Metabolic counterpart of decreased apparent diffusion coefficient during hyperacute ischemic stroke: a brain proton magnetic resonance spectroscopic imaging study." Stroke 34(7): e82-7.

Ohab JJ, Fleming S, Blesch A, Carmichael ST. (2006). "A neurovascular niche for neurogenesis after stroke." J Neurosci 26(50): 13007-16.

Ott A, Breteler MM, van Harskamp F, Stijnen T, Hofman A. (1998). "Incidence and risk of dementia. The Rotterdam Study." Am J Epidemiol 147(6): 574-80.

Pereira JA, Benninger Y, Baumann R, Gonçalves AF, Ozçelik M, Thurnherr T, Tricaud N, Meijer D, Fässler R, Suter U, Relvas JB. (2009). "Integrin-linked kinase is required for radial sorting of axons and Schwann cell remyelination in the peripheral nervous system." J Cell Biol 185(1): 147-61.

Pfaffl, M. W. (2001). "A new mathematical model for relative quantification in real-time RT-PCR." Nucleic Acids Res 29(9): e45.

Piehl F, Lundberg C, Khademi M, Bucht A, Dahlman I, Lorentzen JC, Olsson T. (1999). "Non-MHC gene regulation of nerve root injury induced spinal cord inflammation and neuron death." J Neuroimmunol 101(1): 87-97.

Psaty BM, O'Donnell CJ, Gudnason V, Lunetta KL, Folsom AR, Rotter JI, Uitterlinden AG, Harris TB, Witteman JC, Boerwinkle E; CHARGE Consortium. (2009). "Cohorts for Heart and Aging Research in Genomic Epidemiology (CHARGE) Consortium: Design of

prospective meta-analyses of genome-wide association studies from 5 cohorts." Circ Cardiovasc Genet 2(1): 73-80.

Raben N, Lu N, Nagaraju K, Rivera Y, Lee A, Yan B, Byrne B, Meikle PJ, Umapathysivam K, Hopwood JJ, Plotz PH. (2001). "Conditional tissue-specific expression of the acid alpha-glucosidase (GAA) gene in the GAA knockout mice: implications for therapy." Hum Mol Genet 10(19): 2039-47.

Ransom BR, Stys PK, Waxman SG. (1990). "The pathophysiology of anoxic injury in central nervous system white matter." Stroke 21(11 Suppl): III52-7.

Raphael, A. R. and W. S. Talbot "New insights into signaling during myelination in zebrafish." Curr Top Dev Biol 97: 1-19.

Risch, N. (2001). "The genetic epidemiology of cancer: interpreting family and twin studies and their implications for molecular genetic approaches." Cancer Epidemiol Biomarkers Prev 10(7): 733-41.

Rosamond W, Flegal K, Friday G, Furie K, Go A, Greenlund K, Haase N, Ho M, Howard V, Kissela B, Kittner S, Lloyd-Jones D, McDermott M, Meigs J, Moy C, Nichol G, O'Donnell CJ, Roger V, Rumsfeld J, Sorlie P, Steinberger J, Thom T, Wasserthiel-Smoller S, Hong Y; American Heart Association Statistics Committee and Stroke Statistics Subcommittee. (2007). "Heart disease and stroke statistics--2007 update: a report from the American Heart Association Statistics Committee and Stroke Statistics Subcommittee." Circulation 115(5): e69-171.

Ross, R. (1999). "Atherosclerosis--an inflammatory disease." N Engl J Med 340(2): 115-26.

Ruchoux, M. M. and C. A. Maurage (1998). "Endothelial changes in muscle and skin biopsies in patients with CADASIL." Neuropathol Appl Neurobiol 24(1): 60-5.

Ruijter JM, Ramakers C, Hoogaars WM, Karlen Y, Bakker O, van den Hoff MJ, Moorman AF. (2009). "Amplification efficiency: linking baseline and bias in the analysis of quantitative PCR data." Nucleic Acids Res 37(6): e45.

Schmittgen, T. D. and B. A. Zakrajsek (2000). "Effect of experimental treatment on housekeeping gene expression: validation by real-time, quantitative RT-PCR." J Biochem Biophys Methods 46(1-2): 69-81.

Schneweis S, Grond M, Staub F, Brinker G, Neveling M, Dohmen C, Graf R, Heiss WD. (2001). "Predictive value of neurochemical monitoring in large middle cerebral artery infarction." Stroke 32(8): 1863-7.

Seric, V. (2009). "Possibilities for rehabilitation after stroke." Acta Clin Croat 48(3): 335-9.

Seshadri S, Beiser A, Pikula A, Himali JJ, Kelly-Hayes M, Debette S, DeStefano AL, Romero JR, Kase CS, Wolf PA. "Parental occurrence of stroke and risk of stroke in their children: the Framingham study." Circulation 121(11): 1304-12.

SHAW CM, ALVORD EC Jr, BERRY RG. (1959). "Swelling of the brain following ischemic infarction with arterial occlusion." Arch Neurol 1: 161-77.

Shinton, R. and G. Beevers (1989). "Meta-analysis of relation between cigarette smoking and stroke." Bmj 298(6676): 789-94.

Siebler M, Kleinschmidt A, Sitzer M, Steinmetz H, Freund HJ. (1994). "Cerebral microembolism in symptomatic and asymptomatic high-grade internal carotid artery stenosis." Neurology 44(4): 615-8.

Simard JM, Kahle KT, Gerzanich V. "Molecular mechanisms of microvascular failure in central nervous system injury--synergistic roles of NKCC1 and SUR1/TRPM4." J Neurosurg 113(3): 622-9.

Skoog I, Nilsson L, Palmertz B, Andreasson LA, Svanborg A. (1993). "A population-based study of dementia in 85-year-olds." N Engl J Med 328(3): 153-8.

Spolidoro M, Sale A, Berardi N, Maffei L. (2009). "Plasticity in the adult brain: lessons from the visual system." Exp Brain Res 192(3): 335-41.

Stenzel-Poore MP, Stevens SL, King JS, Simon RP. (2007). "Preconditioning reprograms the response to ischemic injury and primes the emergence of unique endogenous neuroprotective phenotypes: a speculative synthesis." Stroke 38(2 Suppl): 680-5.

Svensson LG, Cruz H, Sun J, D'Agostino S, Williamson WA, Shahian DM. (1996). "Timing of surgery after acute myocardial infarction." J Cardiovasc Surg (Torino) 37(5): 467-70.

Swillens S, Dessars B, Housni HE. (2008). "Revisiting the sigmoidal curve fitting applied to quantitative real-time PCR data." Anal Biochem 373(2): 370-6.

Taguchi A, Soma T, Tanaka H, Kanda T, Nishimura H, Yoshikawa H, Tsukamoto Y, Iso H, Fujimori Y, Stern DM, Naritomi H, Matsuyama T. (2004). "Administration of CD34+ cells after stroke enhances neurogenesis via angiogenesis in a mouse model." J Clin Invest 114(3): 330-8.

Tajouri L, Fernandez F, Griffiths LR. (2007). "Gene expression studies in multiple sclerosis." Curr Genomics 8(3): 181-9.

Thomalla G, Hartmann F, Juettler E, Singer OC, Lehnhardt FG, Köhrmann M, Kersten JF, Krützelmann A, Humpich MC, Sobesky J, Gerloff C, Villringer A, Fiehler J, Neumann-Haefelin T, Schellinger PD, Röther J; Clinical Trial Net of the German Competence Network Stroke. "Prediction of malignant middle cerebral artery infarction by magnetic resonance imaging within 6 hours of symptom onset: A prospective multicenter observational study." Ann Neurol 68(4): 435-45.

Thomalla GJ, Kucinski T, Schoder V, Fiehler J, Knab R, Zeumer H, Weiller C, Röther J. (2003). "Prediction of malignant middle cerebral artery infarction by early perfusion- and diffusion-weighted magnetic resonance imaging." Stroke 34(8): 1892-9.

Thored P, Wood J, Arvidsson A, Cammenga J, Kokaia Z, Lindvall O. (2007). "Long-term neuroblast migration along blood vessels in an area with transient angiogenesis and increased vascularization after stroke." Stroke 38(11): 3032-9.

Thrift AG, Dewey HM, Macdonell RA, McNeil JJ, Donnan GA. (2001). "Incidence of the major stroke subtypes: initial findings from the North East Melbourne stroke incidence study (NEMESIS)." Stroke 32(8): 1732-8.

Tu, I. P. and A. S. Whittemore (1999). "Power of association and linkage tests when the disease alleles are unobserved." Am J Hum Genet 64(2): 641-9.

Turski L, Huth A, Sheardown M, McDonald F, Neuhaus R, Schneider HH, Dirnagl U, Wiegand F, Jacobsen P, Ottow E. (1998). "ZK200775: a phosphonate quinoxalinedione AMPA antagonist for neuroprotection in stroke and trauma." Proc Natl Acad Sci U S A 95(18): 10960-5.

Uyttenboogaart M, Koch MW, Stewart RE, Vroomen PC, Luijckx GJ, De Keyser J. (2007). "Moderate hyperglycaemia is associated with favourable outcome in acute lacunar stroke." Brain 130(Pt 6): 1626-30.

Viader A, Golden JP, Baloh RH, Schmidt RE, Hunter DA, Milbrandt J. "Schwann cell mitochondrial metabolism supports long-term axonal survival and peripheral nerve function." J Neurosci 31(28): 10128-40.

Viitanen, M. and H. Kalimo (2000). "CADASIL: hereditary arteriopathy leading to multiple brain infarcts and dementia." Ann N Y Acad Sci 903: 273-84.

Waxham MN, Grotta JC, Silva AJ, Strong R, Aronowski J. (1996). "Ischemia-induced neuronal damage: a role for calcium/calmodulin-dependent protein kinase II." J Cereb Blood Flow Metab 16(1): 1-6.

Weiss, K. M. and A. G. Clark (2002). "Linkage disequilibrium and the mapping of complex human traits." Trends Genet 18(1): 19-24.

Wise RJ, Bernardi S, Frackowiak RS, Jones T, Legg NJ, Lenzi GL. (1982). "Measurement of regional cerebral blood flow, oxygen extraction ratio and oxygen

utilization in stroke patients using positron emission tomography." Exp Brain Res Suppl 5: 182-6.

Wolf PA, Abbott RD, Kannel WB. (1991). "Atrial fibrillation as an independent risk factor for stroke: the Framingham Study." Stroke 22(8): 983-8.

Wolf, P. A. and J. C. Grotta (2000). "Cerebrovascular disease." Circulation 102(20 Suppl 4): IV75-80.

World Health Organization. The World Health Report. 1999. Geneva, Switzerland: WHO;1999.

The World Health Organization MONICA Project (monitoring trends and determinants in cardiovascular disease). A major international collaboration. WHO MONICA Project Principal Investigators. J Clin Epidemiol. 1988;41:105-114.

Zambonin JL, Zhao C, Ohno N, Campbell GR, Engeham S, Ziabreva I, Schwarz N, Lee SE, Frischer JM, Turnbull DM, Trapp BD, Lassmann H, Franklin RJ, Mahad DJ. "Increased mitochondrial content in remyelinated axons: implications for multiple sclerosis." Brain 134(Pt 7): 1901-13.

Zeller JA, Lenz A, Eschenfelder CC, Zunker P, Deuschl G. (2005). "Platelet-leukocyte interaction and platelet activation in acute stroke with and without preceding infection." Arterioscler Thromb Vasc Biol 25(7): 1519-23.

Zhang S, Dailey GM, Kwan E, Glasheen BM, Sroga GE, Page-McCaw A. (2006). "An MMP liberates the Ninjurin A ectodomain to signal a loss of cell adhesion." Genes Dev 20(14): 1899-910.

Zhang, Z. G. and M. Chopp (2009). "Neurorestorative therapies for stroke: underlying mechanisms and translation to the clinic." Lancet Neurol 8(5): 491-500.

Zhao BQ, Tejima E, Lo EH. (2007). "Neurovascular proteases in brain injury, hemorrhage and remodeling after stroke." Stroke 38(2 Suppl): 748-52.Zhang, S., G. M. Zhang S, Dailey GM, Kwan E, Glasheen BM, Sroga GE, Page-McCaw A. (2006). "An MMP liberates the Ninjurin A ectodomain to signal a loss of cell adhesion." Genes Dev 20(14): 1899-910.

Zhang, Z. G. and M. Chopp (2009). "Neurorestorative therapies for stroke: underlying mechanisms and translation to the clinic." Lancet Neurol 8(5): 491-500.

Zhao BQ, Tejima E, Lo EH.. (2007). "Neurovascular proteases in brain injury, hemorrhage and remodeling after stroke." Stroke 38(2 Suppl): 748-52.

VITAE

Name of author: Antonio Joel Tito

Date and place of birth: February 5, 1987. Pucallpa, Peru

High School: Class of 2005 –

Westchester Academy for International Studies, Houston, TX

Undergraduate: B.S. in Biotechnology, *Magna Cum Laude*

University of Houston - Downtown, December 2008

Post-graduate: University of Texas at Houston Health Science Center. Brown Foundation, Institute of Molecular Medicine. Graduate School of Biomedical Sciences (MS Program)